Evaluating metabolism-induced toxicity using a non-hepatic cell line

Thesis submitted in fulfillment of the requirement for the degree of

Master of Science (Pharmacy)

of

Rhodes University

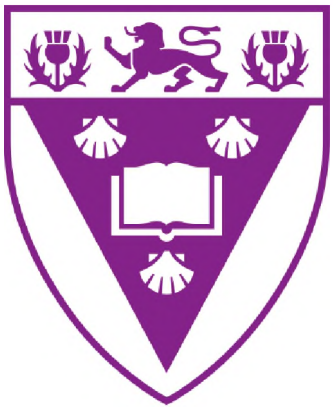

by

Carli Weyers

December 2017

Abstract

The drug discovery pipeline is a complicated process taking roughly 15 years to complete, costing in excess of $1 billion per new chemical entity. It has been estimated that for every 100, 000 promising hit or lead compounds, only one will make it onto the market due to numerous drug candidates being discarded because of many complications. One such complication is metabolism-induced toxicity. Accordingly, an early understanding of the metabolism of any new chemical entity is becoming an integral part of the pipeline. In order to explore this, various methods have been developed including *in silico* and *in vitro* techniques. One such method involves performing cell viability assays on human liver cancer cell lines, which overexpress specific metabolic cytochrome P450 enzymes. If a toxic metabolite is produced it would result in reduced cell viability of the transformed cell line in comparison to a control. Since the liver is the primary site of metabolism in the human body, we were curious as to the extent to which background metabolism may play a role in the degree to which toxic metabolites would be produced in these cell lines. The aim of this project, therefore, was to establish if a non-hepatic cell-based system which overexpresses CYP3A4 could be used to detect the metabolism and any subsequent toxicity of compounds which have been reported to be substrates of the CYP450 enzyme. The HEK293 cell line was stably transfected with a plasmid vector for human CYP3A4 to create a model overexpression system for our metabolism studies. The activity of the enzyme was confirmed using the substrate, 7-benzyloxy-4-trifluoromethyl-coumarin. Subsequently, cytotoxicity testing was done on four known pharmaceuticals reported to generate toxic metabolites in hepatic cell-based assays. *In silico* metabolic predictions on the four known compounds were performed and compared to the results of published literature. Finally, the metabolism of one compound was studied using a combination of high performance liquid chromatography (HPLC) and liquid chromatography-mass spectrometry (LC-MS) in order to detect predicted metabolites. We observed no change in cellular toxicity nor did we detect the formation of metabolites, even though the overexpressed CYP3A4 enzyme was active. The results suggest that caution should be taken when interpreting the results of cell-based metabolism studies, and background metabolism may play a significant role in the data.

Thesis declaration

I declare that this thesis is my own, unaided work. It is being submitted for the degree of Master of Science of Rhodes University. It has not been submitted before for any degree or examination at any other university.

Carli Weyers

December 2017

Table of Contents

List of Figures and Schemes

List of Equations

List of Tables

List of Abbreviations

^{1}H NMR	Proton nuclear magnetic resonance
ADME	Absorption, distribution, metabolism and excretion
ADR	Adverse drug reaction
bp	Base pairs
˚C	Degrees Celsius
cAMP	Cyclic adenosine monophosphate
CMV	Cytomegalovirus
CYP450	Cytochrome P450
δ	Chemical shift
d	Doublet
dd	Doublet of doublets
DCM	Dichloromethane
DILI	Drug-induced liver injury
DMSO	Dimethyl sulfoxide
DNA	Deoxyribonucleic acid
E. coli	*Escherichia coli*
EDTA	Ethylenediaminetetraacetic acid
EET	Epoxyeicosatrienoic acid
EIC	Extracted ion chromatograms
EtOAc	Ethyl acetate
FDA	Food and Drug Administration

FL	Fluorescence
G1 phase	Gap 1 phase
HA tag	Human influenza hemagglutinin tag
HEK293	Human embryonic kidney cells 293
HIV/AIDS	Human immunodeficiency virus infection and acquired immune deficiency syndrome
HPLC	High-performance liquid chromatography
HRP	Horseradish peroxidase
HTS	High-throughput screening
IC_{50}	Median inhibitory concentration
J	Coupling constant
JNK	C-Jun N-terminal kinase
LC-MS	Liquid chromatography-mass spectrometry
LOD	Limit of detection
LOQ	Limit of quantification
m	Multiplet
mg	Milligram
MHz	Megahertz
min	Minute
ml	Mililitre
mmol	Millimolar
MAO	Monoamine oxidase
MKP-1	MAP kinase phosphotase-1

MTT	(3-(4,5-Dimethylthiazol-2-yl)-2,5-diphenyltetrazolium bromide
MW	Molecular weight
NADPH	Nicotinamide adenine dinucleotide phosphate
NCBI	National Center for Biotechnology Information
NHBE	Normal human bronchial epithelial cells
NMR	Nuclear magnetic resonance
PBS	Phosphate buffered saline
PDA	Photo diode-array
RNA	Ribonucleic acid
ROS	Reactive oxygen species
rpm	Revolutions per minute
SAR	Structure activity relationship
SDS	Sodium dodecyl sulphate
s	Singlet
S phase	Synthesis phase
SMILES	Simplified molecular-input line-entry system
TAE	Tris-acetate-EDTA buffer
THLE	Transformed human liver epithelial cells
TLC	Thin layer chromatography
t	Triplet
µg	Microgram
µl	Microlitre
UV	Ultraviolet

Acknowledgements

First and foremost, I want to thank my supervisors Dr. Clint Veale and Prof. Adrienne Edkins from the bottom of my heart for all their encouragement over the past two years. Their guidance in this project has been instrumental and I could not possibly have asked for two better supervisors for my Master's thesis. Thank you both for the time and never-ending support you have given me throughout this thesis.

I would also like to thank Dr. Brendan Wilhelmi and Dr. Sagaran Aboo for their help with the HPLC chapter of this thesis. Without them this section of my thesis would not have been possible. I particularly want to thank Dr. Wilhelmi for always being available and answering my seemingly endless amount of questions.

Thank you to my parents for supporting me throughout my university career (both financially and emotionally) and creating a love for science in me from a young age which has been the stepping stones in getting me where I am today. Words cannot explain how appreciative I am of everything you have done for me.

To my loving boyfriend Amaury, thank you so much for always supporting me and showing such deep interest in my work and progress even though you might not always have known what I was doing.

Thank you so much to my colleagues in both BioBRU and the pharmaceutical chemistry labs! I am so extremely blessed and grateful to have been a part of two such amazing labs and been able to work with such talented scientists. Without your help with my experiments and encouragement when I needed it most I would not have been able to survive these past two years. Special thanks need to be extended to Ms. Laura M.K. Dingle, Dr. Jason Neville Sterrenberg, Ms. Shantal Maharaj, Mr. Mayibongwe Lunga, Ms. Lissa Ruramai Chisango, Mr. Donovan Nel, Dr. Sarah Kituyi, (Dr.) Stacey Mattison and Ms. Kelly Schwarz.

Lastly, I would like to gratefully acknowledge the NRF for the Innovations and Scarce Skills Scholarship which funded the second year of my M.Sc.

Research Outputs

Conferences

Carli Weyers, Laura M.K. Dingle, Adrienne L. Edkins, Clinton G.L. Veale. (2016). *In vitro* oxidative metabolic profiling of novel anti-plasmodial agents. All Africa Congress on Pharmacology and Pharmacy. Muldersdrift, Gauteng. POSTER PRESENTATION

Carli Weyers, Laura M.K. Dingle, Adrienne L. Edkins, Clinton G.L. Veale. (2016). *In vitro* oxidative metabolic profiling of novel anti-plasmodial agents. Frank Warren Organic Chemistry Conference. Grahamstown, Eastern Cape. FLASH PRESENTATION AND POSTER PRESENTATION

CHAPTER 1
LITERATURE REVIEW

Early drug discovery processes

Drug discovery is defined as the process by which a drug candidate is identified and validated in order to treat a certain disease. This definition does not include preclinical studies, clinical trials and regulatory approval, such as the Food and Drug Administration (FDA) (Goulding & Marden, 2009). The process of developing a new drug from start to finish can cost more than $1 billion and take about 12-15 years to complete (Hughes, Rees, Kalindjian, & Philpott, 2011). The drug discovery process is extensive and consists of several phases and steps, which include choosing a disease, choosing a drug target, identifying a bioassay, lead identification, optimizing target interactions and optimizing access to the target (Maurer, 2006).

The first step is choosing a disease. This step is critical because pharmaceutical companies must make a profit and extract the maximum value for every dollar which they spend on the research (Maurer, 2006). Therefore, they will most likely avoid diseases which only affect a small subgroup of the population and diseases which affect patients of lower economic status (Ridley, Grabowski, & Moe, 2006). Usually research is focused on non-communicable diseases which affect first world countries. However, recently more focus has been placed on neglected diseases prevalent in third world countries. These diseases include tuberculosis, malaria, HIV/AIDS and trypanosomiasis (Maurer, 2006).

The next step in the process is identifying a biological target. This can originate from a variety of sources such as academic and clinical research (Hughes et al., 2011) and includes a wide range of biological entities such as genes, proteins and RNA (Schenone, Dančík, Wagner, & Clemons, 2013). This step requires a definitive understanding of the disease mechanism in order to identify any drug targets. For example, HIV proteases can be the targets as these are important for HIV replication (Goulding & Marden, 2009). In addition, in order to select a viable biological target, genomics and proteomics could be explored as these techniques provide valuable information with regards to the global gene expression in diseased tissue as opposed to normal tissue. The determined target requires further validation before it is possible to move into the hit and lead discovery drug phases. This validation is imperative in order to prove that a drug discovery effort is necessary (Sacks et al., 2014).

After target validation, compound screening assays are developed, followed by hit compound identification. Once a hit has been identified, it is optimized in order to identify a structure activity relationship (SAR) and begin establishing the possible pharmacophore, resulting in a lead compound (Hughes et al., 2011) (Keserű & Makara, 2006). The lead optimization phase is characterized by a multifactorial optimization and the drug candidate is advanced in terms of potency, selectivity, physiochemical properties, administration, distribution, metabolism, and excretion (ADME) and reducing toxicity (Keserű & Makara, 2006). These studies make it possible to select compounds which can potentially be developed into pre-clinical candidates, which can be evaluated in clinical trials to deliver approved drugs considered to be safe and effective (Goulding & Marden, 2009).

This description of the drug discovery pipeline may give the impression that it is a routinely successful process. However, this process suffers from a high rate of attrition, which is compounded by a lack of in-depth metabolic profiling in the early stages (J. Wang & Urban, 2004).

Importance of metabolism

Two of the biggest challenges in drug development are bioavailability and toxicity, both of which are influenced, in part, by metabolism (Guengerich, 2006). A lack of understanding of the metabolic processes of drugs early in the drug discovery pipeline could potentially result in unforeseen complications of candidate molecules and their subsequent rejection from the pipeline. Therefore, exploring this aspect of drug discovery at a much earlier stage of development has become an important element to inform SAR interpretations and lead selection, hopefully, leading to a reduction in the failure rates of potential drugs (Park, Williams, Naisbitt, Kitteringham, & Pirmohamed, 2005). As part of this metabolic profiling, it is important to understand the effect that metabolic enzymes, like the CYP450 enzyme family, may have on any new active compounds, particularly with regards to half-life, duration of action and toxic or active metabolites in order to inform the hit and lead optimization stages (Crespi & Stresser, 2000).

In some instances, metabolism results in the bioactivation of drugs to form reactive intermediate metabolites through reaction with CYP450 enzymes. These metabolites can have physiochemical and pharmacological properties which are different to that of the parent drug which means that there could

be major implications with regards to the safety and efficacy of a particular drug (Kirchmair et al., 2015). These metabolites can often lead to toxicity which causes adverse drug reactions (ADRs) (Guengerich, 2006). This toxicity can result in oxidation of cellular components or the inhibition of normal cellular functions. Therefore, *in vitro* models are essential in establishing basic mechanisms of metabolism and studying bioactivation. However, bioactivation is only one context of toxicity and it is important to determine what fraction of drugs fall out of the drug discovery pipeline due to the presence of toxic metabolites (Guengerich, 2006). An analysis by Pfizer concluded that 62% of the drugs withdrawn from the market, as a result of human drug toxicity problems were due to metabolism-related issues and in particular, the presence of reactive metabolites (Guengerich, 2006). This analysis only encompassed drugs which reached the market and therefore the fraction may be higher as many drugs are rejected before entering clinical trials and safety assessments.

An excellent example of a drug associated with toxic metabolites is the general anesthetic halothane, the extensive biotransformation of which results in reactive metabolites which cause hepatotoxicity (Spracklin, Hankins, Fisher, Thummel, & Kharasch, 1997). In this case there is direct experimental data which links metabolic activation with clinical symptoms of hypersensitivity. About 20-50% of halothane is converted by CYP2E1 to a reactive intermediate metabolite, trifluoroacetyl chloride, which binds to certain liver proteins (Park et al., 2005). The resultant neoantigens stimulate an immune reaction, resulting in severe liver necrosis. However, by modifying the structure of the compound it was possible to decrease the incidence of hepatotoxicity by almost 95% (Park et al., 2005).

Another example is sulfamethoxazole which is an antibacterial agent but has been shown to cause severe immunological problems such as anaphylaxis and Stevens-Johnson syndrome. The toxicity associated with sulfamethoxazole has been attributed to its oxidation into a nitroso-sulfamethaxazole metabolite by CYP450 (**Scheme 1**). In this metabolic pathway, sulfamethoxazole is metabolized to the sulfamethoxazole hydroxylamine and further oxidized by CYP450 enzymes to nitroso-sulfamethaxozole (**Scheme 1**) (Spracklin et al., 1997). The final metabolite is reactive, resulting in haptenation of cellular protein and subsequent hypersensitivity reactions (Park et al., 2005). These examples demonstrate how toxic metabolites can be formed from various non-toxic functional groups in the parent compound by normal biotransformations within the body's metabolic system.

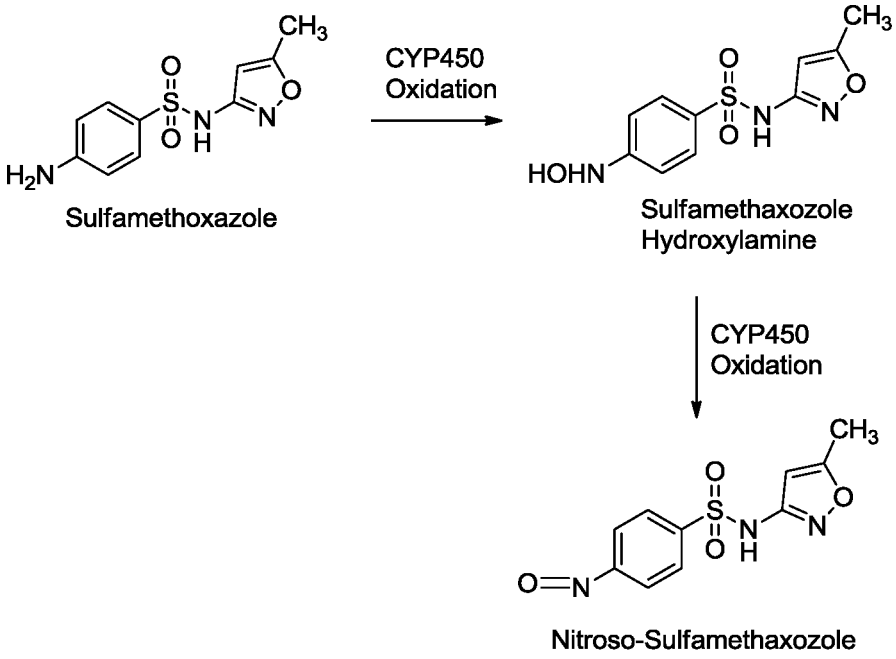

Scheme 1: Sulfamethoxazole metabolism*. Metabolic pathway of sulfamethoxazole as outlined by Spracklin et al. (1997).*

Drug-induced liver injury (DILI) is the most commonly cited reason for drugs being withdrawn from the market after approval. In addition, DILI also accounts for 50% of acute liver failure cases (Park et al., 2005). DILI can result from interactions of drugs and/or their metabolites with biochemical processes which can trigger a protective response or cause tissue injury. DILI and ADRs, in general, present a major concern to the pharmaceutical industry because drug withdrawal during development, or even after approval, represents a substantial loss of investment. Therefore, the study of drug metabolism, pharmacokinetics and toxicokinetics (drug disposition) is imperative in understanding the action of the compound during drug development (Park et al., 2005). In order to accurately assess the benefit and risk ratio of a drug, it is necessary to identify the active metabolites and their concentrations in the plasma and within cells because the final selection of a lead compound depends on the results obtained from drug metabolism studies (Gunaratna, 2000). In conclusion, if metabolism is investigated early in the drug development process, waste of human effort and technical resources can be minimized.

Overview of various metabolic processes

The purpose of drug metabolism is to remove foreign chemicals, also known as xenobiotics, from the body or for recycling (Banerjee & Ghosh, 2016). Generally, this is achieved through the introduction of polar moieties, which increase the hydrophilicity of a given substrate. However, this process can result in the formation of active metabolites. The reactions can be grouped into two general categories namely, Phase 1 and Phase 2 reactions (Banerjee & Ghosh, 2016).

Phase 1 metabolism includes processes such as oxidation, reduction and hydrolysis which are usually catalyzed by Cytochrome P450 (CYP450) enzymes. The reactions that take place during Phase 1 install the functional groups (usually polar) which allow the molecule to undergo Phase 2 metabolism (Gibson & Skett, 2001) (Humma, Ellingrod, & Kolesar, 2003). Phase 2 metabolism involves the addition of a highly hydrophilic molecule, which is naturally present in the body, onto the drug molecule (Gibson & Skett, 2001). This process is known as conjugation. Following this reaction most of the conjugates lose their biological activity, or are detoxified and are then removed from the body via the urine. Common reactions associated with Phase 2 metabolism include glucuronidation, acetylation, methylation, sulfate conjugates, glycine and glutamate conjugates, and glutathione conjugates (Gibson & Skett, 2001).

General information about CYP450 enzymes

CYP450 are haem containing monooxygenase enzymes predominantly expressed in the endoplasmic reticulum of the liver (Ogu & Maxa, 2000). More than fifty CYP450 isoforms are known to exist in the human body. These have been classified into 17 families and 39 subfamilies which are based on similarities in the amino acid sequence (Danielson, 2002). The families have a more than 40% amino acid sequence identity and are designated a number following the abbreviation 'CYP'. The CYP450 enzymes present in a subfamily share more than 60% sequence identity and can be distinguished from each other by a letter following the number (Gunaratna, 2000). The most highly expressed forms are CYP3A4, CYP2C9, CYP2C8, CYP2E1 and CYP1A2 (Ogu & Maxa, 2000). The main monooxygenase function of these enzymes is to introduce oxygen into a molecule, thereby decreasing its lipophilicity which causes the product to be eliminated from the body (Crespi & Stresser, 2000). In other words, these enzymes

catalyze the metabolism of many drugs, through oxidative biotransformation. This biotransformation is complex; however, the overall reaction is represented in **Equation 1.**

$$RH + O_2 + NADPH + H^+ \rightarrow ROH + H_2O + NADP^+$$

Equation 1.1: CYP450 oxidative biotransformation.

These enzymes also initiate the synthesis of organic molecules such as cholesterol, steroids and other lipids. This biotransformation is often the first phase in drug metabolism, the purpose of which is to prepare a xenobiotic for elimination, or deactivate it.

CYP450s generally have a broad substrate specificity which means that each CYP450 enzyme can catalyze the oxidation of a wide variety of drugs, and the metabolism of a drug by CYP450 enzymes could be as a result of one or a variety of different enzymes (Rousu & Timo, 2012). Therefore, identifying the primary metabolic enzyme of a given drug may be difficult. The main consequence of this multiple-substrate metabolism, however, is metabolism-based drug-drug interactions. Therefore, drugs which are co-administered could potentially lead to the induction or inhibition of CYP450 enzymes which metabolize these drugs (Gunaratna, 2000). Enzyme inducers cause an increase in specific enzyme levels by modulating gene expression. It is also possible for drugs to induce CYP450 enzymes which are not involved in their metabolism. For example, the drug omeprazole is metabolized by CYP2C19 and CYP3A4, however, it causes the induction of CYP1A2 (Shih, Pickwell, Guenette, Bilir, & Quattrochi, 1999). Therefore, co-administration of omeprazole with a drug that is generally metabolized by CYP1A2, for example acetaminophen, will decrease the effect of acetaminophen.

Alternately, enzyme inhibitors either competitively or non-competitively inhibit the function of CYP450 enzymes, thereby resulting in reduced elimination or deactivation of a circulating drug. Enzyme induction or inhibition can result in plasma concentrations of a drug which are significantly different from the desired concentration and could lead to failure in treatment and, in extreme cases, cause toxicity which results in adverse effects (Rousu & Timo, 2012). CYP450 enzymes have also been found in the intestinal epithelial cells and here the enzymes significantly affect the amount of drug which is eventually absorbed into systemic circulation. For example, it has been proven that drugs which are

susceptible to metabolism via CYP3A4 could potentially have low or variable bioavailability (Jia & Liu, 2007).

CYP3A4

CYP3A4 is the most prevalent liver enzyme expressed by humans and is responsible for the oxidative metabolism of more than half of all known drugs (Gupta, Hollis, Patel, Patrick, & Bell, 2003). The concentration of CYP3A4 in liver ranges from 47-523 pmol/mg and has been shown to have large inter-individual variation (Patki, Moltke, & Greenblatt, 2003). CYP3A4 has also been found to be expressed in the prostate, breast, gut, colon, small intestine and brain in smaller concentration ranges (Basheer, Kerem, Basheer, & Kerem, 2015). The general CYP450 active site is composed of an iron containing porphyrin ring referred to as the haem iron center which is anchored by four non-covalent bonds (**Figure 2**) (Basheer et al., 2015). This active site is able to accommodate multiple ligands of various sizes. The fold of the CYP450 is highly conserved but despite this it has enough structural variability to allow for binding of different size substrates and with diverse specificity (Baj-Rossi, De, & Carrar, 2011).

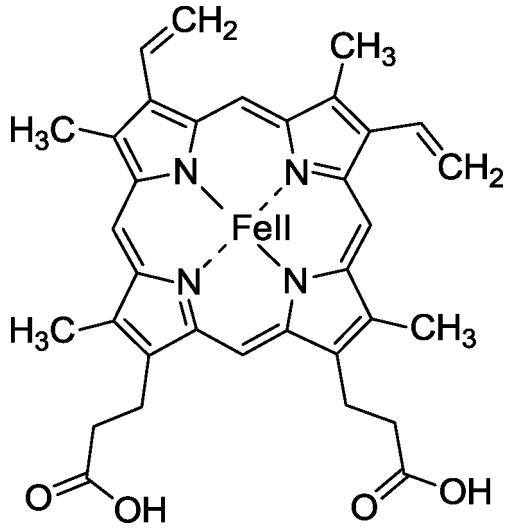

Figure 2: CYP450 haem structure*. Structure of basic CYP450 haem as proposed by Baj-Rossi et al. (2011).*

CYP3A4 is responsible for the metabolism of the highest proportion of pharmaceuticals (Denisov, Makris, Sligar, & Schlichting, 2005). Due to the structural diversity of CYP3A4 it is difficult to predict the metabolism and potential drug interactions of lead compounds (Scott & Halpert, 2005).

Computational methods of ADME prediction

Determining the ADME properties of a drug is imperative in the drug discovery process. More precisely, however, the site of metabolism, as well as the rate and extent of metabolism and the number of metabolic pathways are some of the most critical pharmacokinetics of a drug (Crivori & Poggesi, 2006). In recent years, computational methods have been developed to predict drug metabolism with the aim of improving lead selection as well as increasing the pace of progression of leads into drug candidates (Pires, Blundell, & Ascher, 2015).

In silico methods have been developed to make investigations/predictions pertaining to: structure, function and mechanisms of metabolic enzymes, sites of metabolism, metabolites (chemical structure), interactions of drugs with targets related to drug metabolism, bioactivity and toxicological effects and metabolite identification (Kirchmair et al., 2015). However, each method has its own set of limitations with the key to using these methods being integration of multiple techniques and resources (Crivori & Poggesi, 2006). Computational methods are based on experimental data in which conditions and variables are kept constant. This means it does not take into account any variability, especially in *in vivo* conditions which often results in these models being incomplete (Kirchmair et al., 2015). **Table 1** below outlines the various computational methods in use and the scope/limitations of these methods which provides valuable insight into the drawbacks of *in silico* prediction. Even though this approach has its shortcomings, it is possible to make use of biotransformation data to predict sites and products of metabolism. For example, a program MetaPrint2D is able to predict sites of metabolism by making use of biotransformation databases. This method does however have limited applicability because it requires thousands of biotransformation data in order to predict proper model development and with the current scarcity of data this method is highly impractical (Kirchmair et al., 2015). This is just one example of the limitations of computational methods because it is still a relatively young field of research. Therefore, it is imperative to combine different experimental and theoretical approaches in order to generate a clear picture of the metabolism of a specific compound (Kirchmair et al., 2015). A synergy in computational and experimental methods will allow the analysis/prediction of drug metabolism to accelerate rather than looking at these two approaches separately (Kirchmair et al., 2015).

Table 1: Various computational methods. Scope and limitations of computational methods copied with permission from Kirchmair et al. (2015).

Investigation/prediction of	Computational method(s)	Scope, limitations
Structure, function and mechanisms of metabolic enzymes	Homology modelling, quantum mechanics, molecular dynamics simulations etc.	Analysis of ligand binding events and enzyme mechanisms at a high level of detail and accuracy. Particularly useful for the investigation of unstable reaction intermediates with very short lifetimes.
Sites of metabolism	Knowledge-based systems, data mining, machine learning, QSAR models, reactivity models, ligand docking, molecular interaction fields, shape-based methods etc.	Able to predict the likely SoMs (metabolic liabilities) with adequate accuracy: In general, at least one SoM is correctly identified among the three highest-ranked atom positions of a molecule in 70-90 % of all cases within the domain of chemical applicability.
Metabolites (chemical structure)	Knowledge-based systems, data mining	Dominated by knowledge-based systems. Can produce large numbers of metabolites. Main challenge: finding ways of ranking metabolites accurately.
Metabolic rates	Quantum mechanics, molecular dynamics simulations, (QSAR models)	Prediction generally not possible. Only within extremely narrow chemical space QSAR-like approaches may work.
Interactions of drugs with targets related to2drug metabolism	QSAR models	Prediction of ligand affinity and inhibitory activity where adequate training data is available. Prediction of mechanism-based inhibitors remains highly challenging.
	Free energy calculations	Accurate prediction of binding affinities without need for extensive training data. Computationally expensive and labour-intense.
Bioactivity and toxicological effects	Various ligand- and structure-based approaches	Target prediction methods have become abundantly available but high false positives rates (i.e. accurate ranking of targets) remain a limiting factor. Prediction of bioactivities for metabolites hampered by lack of training data. Rule-based approaches are able to detect most toxicophores, but prediction of time-dependent inhibitors remains challenging.
Metabolite identification (MetID)	Various metabolite generation and spectra analysis approaches	Has seen major advances in recent years, driven by increasingly available data, data exchange and new algorithms. Major scientific instruments manufacturers offer bespoke MetID software. Vendor-independent and open-source packages are becoming increasingly available.

In vitro models of metabolism

Technologies used to assess *in vitro* liver metabolism vary from whole liver to subcellular models, producing information on metabolic substrate as well as inhibitor specificity of metabolic enzymes (Fasinu, Bouic, & Rosenkranz, 2012). Specific technologies in this area of research include isolated fresh liver, liver slices, hepatocytes, microsomes, cytosolic fractions and purified or heterologously expressed drug-metabolizing enzymes (Fasinu et al., 2012). Even though each of these methods have their own set of advantages and limitations, the choice of method will depend on the research question to be answered as well as the relevance to man, influence of test drugs on enzyme activity and the metabolites formed (Fasinu et al., 2012). From the abovementioned methods, hepatocytes and liver slices are the most physiologically relevant as they most closely resemble *in vivo* conditions. These methods have been used successfully in previous studies (Du et al., 2014) (Guillén et al., 1998). A study conducted by Yamane et al. (2015) explored the metabolism of tofogliflozin, a sodium-glucose co-transporter 2 inhibitor, by making use of human liver microsomes, human hepatocytes and recombinant human CYP450. In this study the use of human hepatocytes yielded metabolites which were the same as those identified from *in vivo* conditions. However, the use of these human hepatocytes are limited due to the "restricted access to suitable tissue samples" (Gomez-Lechon, Donato, Castell, & Jover, 2003) because the samples lose viability exceedingly quickly and fresh liver samples are not readily available. In addition, there is a high cost and variability between samples associated with human hepatocytes making their use impractical (Vignati et al., 2005).

As a result of these limitations, advances have been made in alternative cellular models such as cells which stably express individual CYP450 enzymes (Gomez-Lechon et al., 2003). A study by Vignati et al. (2005) combined human CYP3A4 with their HepG2 target cells by either incubating the CYP3A4 containing microsomes with the HEPG2 cells or transiently transfecting the cells with CYP3A4. In both these methods the CYP3A4 was deemed active through the metabolism of test compounds, and was expressed in levels comparable to that of hepatocytes (Vignati et al., 2005). The use of stable cell lines expressing CYP450s is preferred, however, over transient transfections because the whole process of metabolism and subsequent toxicological consequences all happen in the same cells (Sawadaa & Kamatakib, 1998). These stably transfected cell lines have made it possible, in *in vitro* settings, to test the toxicology of a chemical (Sawadaa & Kamatakib, 1998). Various cell lines have been used in multiple

studies to test various aspects of toxicology such as mutation, cytotoxicity and metabolism. The choice of the recipient cell line is an important factor to consider. The use of AHH-1 and Chinese hamster cell lines have been used numerous times. However, a number of other human cells such as HeLa (cervical carcinoma), HepG2, MCF-7 (mammary carcinoma), BEAS-2B (bronchial epithelial cells) and HEK293 (kidney epithelial) have been used successfully (Sawadaa & Kamatakib, 1998). The choice of cell line should eventually depend on whether the cell line has other factors present which are essential for the function of the CYP450 enzyme and also the purpose of these genetically engineered cells (Sawadaa & Kamatakib, 1998).

Knowledge Gap

The drug discovery process is highly complex, taking about 12-15 years to complete and costing over $1 billion (Hughes et al., 2011). The process consists of several phases, including choosing a disease, choosing a drug target, identifying a bioassay, lead identification, optimizing target interactions and optimizing access to the target (Maurer, 2006). However, this process suffers from high rates of attrition, with numerous promising candidates falling out at various stages of the pipeline. Unidentified metabolic toxicity of late stage lead compounds has been identified as one reason for this. Accordingly, metabolic profiling and the identification of toxic metabolites is becoming an important consideration early in the pipeline. One option available is the evaluation of metabolism using *in vitro* cell based systems expressing CYP450 enzymes (Patki et al., 2003). However, the influence of background metabolism inherent in liver cells has yet to be tested, a factor which may well alter the results obtained by these studies. Therefore, this project aims to investigate published *in vitro* methods using reported CYP3A4 substrates against a cell line which overexpresses CYP3A4. The single exception is that in place of a hepatic cell line, we used a kidney cell line (HEK293) in order to evaluate the background influence. Furthermore, we aimed to compare these results to published literature and *in silico* predictions of metabolism in order to determine the validity in using these methods to ascertain drug metabolism.

Research Question

Can a non-hepatic cell-based system with CYP3A4 overexpression be used to detect the metabolism and toxicity of reported CYP3A4 substrates?

Aims

1. *In silico* profiling of metabolism in comparison to results reported by literature.
2. Creation and validation of a HEK293 cell line stably expressing CYP3A4 (and the equivalent control).
3. Conducting metabolism studies of previously experimented known compounds using the CYP3A4-expressing cell line created in (2)

CHAPTER 2
MATERIALS AND METHODS

Materials

Molecular and Tissue Culture Reagents

Dulbecco's Modified Eagle's medium (DMEM), Opti-MEM® and Fetal bovine serum (FBS) were purchased from Life Technologies/Gibco (Invitrogen). The Geneticin (G418) sulphate was from Santa Cruz Biotechnology. The *Nhe*I and *Xho*I restriction enzymes, Quick load 1kb DNA ladder and blue prestained protein standard broad range ladder were from New England Biolabs. The gDNA mini prep kit and the Zyppy ™ Plasmid Miniprep Kit were from Zymo Research. The EndoFree Plasmid Maxi Kit was from Qiagen. The Blue Prestained molecular weight ladder was from Thermo Scientific. The anti-HA tag antibody - ChIP grade (AB9110) was from Biocom Africa. The X-tremeGENE HP DNA transfection reagent and Cell Proliferation Kit I for MTT assays were purchased from Roche (Sigma-Aldrich). The sodium pyruvate, trypsin, accutase, trypan blue, ampicillin, protein inhibitor cocktail, nicotinamide adenine dinucleotide phosphate (NADPH), perchloric acid, propranolol, labetalol, chlorpromazine, rosiglitazone, resorcinol and ethyl 4,4,4-trifluoroacetoacetate were purchased from Sigma-Aldrich. All other materials were purchased from Sigma-Aldrich or SAARCHEM (Merck).

High performance liquid chromatography (HPLC) reagents

All chemicals used in these analyses were of HPLC grade. Triethylamine and acetonitrile gradient grade for liquid chromatography LiChrosolv® were purchased from Sigma-Aldrich. Sodium dihydrogen orthophosphate dihydrate and ortho-phosphoric acid (85 %) analytical grade were purchased from Merck Laboratories. Propranolol and labetalol were donated by Prof. Roderick Walker (Rhodes University Pharmacy Faculty).

Methods

In silico metabolism prediction

Main metabolites were predicted using the ChemAxon JChem Metabolizer software (https://www.chemaxon.com/products/metabolizer/). This software makes use of a biotransformation library consisting of generic reactions. pkCSM (predicting small-molecule pharmacokinetic and toxicity properties using graph-based signatures) software was used to predict the most likely drug metabolizing enzymes
(http://biosig.unimelb.edu.au/pkcsm/prediction) (Pires et al., 2015).

General chemistry

NMR spectra were acquired using either Bruker Fourier 300 or a 600 MHz Avance II spectrometer. Chemical shifts are reported in ppm, referenced to residual solvent resonances ($(CH_3)_2CO$-d6 δH 2.04; DMSO-d6 δH 2.50). High resolution mass spectrometry was performed on a Waters Synapt G2 TOF instrument with an ESI source.

Synthesis of 7-benzyloxy-4-trifluoromethyl coumarin substrate for CYP3A4

Procedure for the synthesis of 7-hydroxy-4-trifluoromethyl-2H-chromen-2-one

A catalytic quantity of molecular iodine (20 mol%, 1.2 mmol) was added to a stirring solution of resorcinol (275.25 mg, 5 mmol) and ethyl-4,4,4-trifluoroacetoacetate (440 µl, 6 mmol) in toluene (0.5 ml) and heated to 90 °C. Following constant monitoring via TLC the reaction was stopped at 4 hours and allowed to cool to room temperature. The solution was diluted with EtOAc (10 ml) and washed with water (2 x 20 ml) and brine (2 x 20 ml) and dried over anhydrous $MgSO_4$. The solvent was removed *in vacuo* and the reaction was purified using normal phase flash chromatography (Hex: EtOAc 4:1). This synthesis used was a modification of the methods used by DeGrote, Tyndall, Wong, & VanAlstine-Parris (2014) and Tyndall, Wong, & VanAlstine-Parris (2015).

General procedure for the synthesis of 7-benzyloxy-4-trifluoromethyl coumarin

Benzyl bromide (151.34 mg, 10 mmol, 2 eq.) was added dropwise to a stirred mixture of the phenol (94.3 mg, 11 mmol) and K_2CO_3 (61.14 mg, 11 mmol) in 20 ml anhydrous acetonitrile. The resulting solution was heated under an atmosphere of nitrogen to reflux (90 °C) and maintained for 3 and a half hours. The reaction mixture was constantly monitored using TLC. Following completion of the reaction, it was allowed to cool to room temperature and diluted with EtOAc (10 ml), washed with water (2 x 20 ml) and brine (2 x 20 ml) and dried over anhydrous $MgSO_4$. The solvent was removed *in vacuo* and the reaction was purified using normal phase flash chromatography (Hex: EtOAc 4:1). This synthesis was a modification of the method used by Velasco, Silva López, Nieto Faza, & Sanz (2016).

Cell lines and culture conditions

The HEK293 (Human Embryonic Kidney; ATCC CRL-1573) cells were a gift from Prof. Heinrich Hoppe (Rhodes University). HEK293 cells were maintained in complete medium composed of Dulbecco's Modified Eagle's Medium (DMEM) supplemented with 10 % (v/v) foetal bovine serum (FBS), 1 % (v/v) GlutaMAX (Gibco, Life Technologies), 0.1 mM Minimum Essential Medium (MEM) non-essential amino acids, 1 mM sodium pyruvate, 1 % (v/v) Antibiotic-Antimycotic solution (100 U/ml penicillin, 100 µg/ml streptomycin, 12.5 µg/ml amphotericin [PSA]). The HEK293-CYP3A4-HA and HEK293-pcDNA3.1+ cell lines were maintained in complete medium with 500 µg/ml G418. The cells were kept at 37 ˚C in a humidified 9 % CO_2 incubator.

Creation of a mammalian expression plasmid to express human CYP3A4

The coding sequence for CYP3A4 was retrieved from NCBI with the reference sequence NM_001202855.2. A Kozak sequence was introduced at the 5' end of the sequence to facilitate translation initiation. In addition, the coding sequence for the human influenza hemagglutinin tag (HA tag) was added in frame with the 3' end of the CYP3A4-coding sequence, just before the stop codon. The CYP3A4 sequence was synthesized by Genscript (Hong Kong) and cloned into the mammalian expression vector pcDNA3.1+ to generate the pcDNA3.1+/CYP3A4-HA expression plasmid.

Plasmid transformation and confirmation via restriction digestion

The pcDNA3.1+/CYP3A4-HA plasmid was transformed into competent *Escherichia coli (E.Coli)* DH5α cells according to the manufacturer's instructions (Addgene) and plated onto 2x Yeast Tryptone (2x YT) (16 g/L tryptone, 10 g/L yeast extract, 5 g/L NaCl, 15 g/L agar) agar plates containing ampicillin (100 µg/ml) for selection of colonies. The plate was incubated at 37 °C overnight, after which single transformed colonies were picked for an agar stab and inoculated into 5 ml of 2x YT broth (16 g/L tryptone, 10 g/L yeast extract, 5 g/L NaCl) containing ampicillin (100 µg/ml). The 5 ml cultures were grown at 37 °C overnight with shaking (180 rpm). The plasmid was extracted using the Zyppy Plasmid Miniprep Kit (Cat #: D4019) according to manufacturer's instructions and DNA concentration quantified by absorbance at 260 nm using the Nanodrop 2000 spectrophotometer. Restriction enzyme digestions of the plasmid using either *Xho*I (Cat #: R0146S) or *Nhe*I (Cat #: R3131S) or both were performed in order to confirm the plasmid identity. The reactions contained 0.25 µg of plasmid DNA, 5 U of each respective restriction enzyme in 1x CutSmart buffer (Cat #: B7204S) in a total volume of 20 µL. The restriction digestion was performed for 2 hours at 37 °C. The reaction was stopped with the addition of 6x DNA loading buffer (60 % [v/v] glycerol, Tris-HCl (pH 7.6) 10 mM, ethylenediaminetetraacetic acid (EDTA), 60 mM, bromophenol blue, 0.03 % [w/v] xylene cyanol ff). Digested and undigested plasmids were visualized on a 1 % (w/v) agarose gel prepared using 1x Tris-acetate-EDTA buffer (TAE, 40 mM Tris acetate, 1 mM EDTA) and ethidium bromide (0.5 µg/ml) after electrophoresis at 120 V for approximately 45 minutes. Images were obtained using the Chemidoc system (Biorad) under UV illumination.

Transfection and generation of polyclonal stable cell lines expressing either pcDNA3.1+/CYP3A4-HA or pcDNA3.1+

Endotoxin-free maxipreps of the pcDNA3.1+/CYP3A4-HA and pcDNA3.1+ plasmids were prepared using the Qiagen Endofree® Plasmid Maxi Kit according to the manufacturer's instructions (Cat #: 12362). The DNA concentrations were measured using absorbance at 260 nm on the NanoDrop2000 spectrophotometer (Thermo Scientific). The endotoxin free preparations of the plasmids were individually transfected into the HEK293 cell line using X-tremeGENE HP DNA Transfection Reagent according to manufacturer's instructions. Briefly, the HEK293 cells were seeded into a 6-well plate in HEK293 media at ±70 % confluency 24 hours before transfection and allowed to adhere overnight at 37

°C in the 9 % CO_2 incubator. At 24 hours after seeding, the cells were transfected with pcDNA3.1+ vectors (2 µg DNA per well) using X-tremeGene HP DNA Transfection Reagent (Roche). Each plasmid was diluted with Opti-MEM I Reduced Serum Media (200 µl). X-tremeGENE HP Transfection Reagent (4 µl) was added and the mixture was incubated for 15 min at 25 ˚C. The transfection mixture was added to the cells (in a dropwise manner) and the plate incubated at 37 °C in a humidified incubator with 9 % CO_2 for 48 hours. After 48 hours the cells were lifted with trypsin and transferred from the 6-well plates into two 10 cm dishes where positive transfectants were selected for in the presence of complete medium containing 500 µg/ml G418. The medium in the dishes was replaced every 3 days. Once visible colonies appeared, the cells were transferred into T25 culture vessels and maintained until they were 100 % confluent or processed for Western blot analysis. The growth of the cells was documented using Zeiss phase contrast light microscope and camera. The resultant stable cell lines were termed HEK293-CYP3A4-HA and HEK293-pcDNA3.1+.

Preparation of cell lysates

Cell lysates were prepared by adding 400 µl of CelLytic™ M (Sigma) to a confluent T25 culture vessel which contained transfected HEK293 cells which had been previously washed with 5 ml of phosphate buffered saline (PBS, 10 mM Na_2HPO_4, 1.8 mM KH_2PO_4, 2.7 mM KCl, 140 mM NaCl, pH 7.4). The vessel was incubated at 4 ˚C on a shaker for 15 min, after which cells were scraped under sterile conditions into the lysis buffer. Protein concentrations of the cell lysates were measured using absorbance at 280 nm on the NanoDrop2000 spectrophotometer (Thermo Scientific) and the lysates used for SDS-PAGE and Western blot analysis.

Sodium dodecyl sulphate polyacrylamide gel electrophoresis (SDS-PAGE) and Western blot analysis

The cell lysates were combined with 100 µl of 5 X SDS sample buffer (0.05 M Tris-HCl pH 6.8, 10 % [v/v] glycerol, 2 % [w/v] SDS, 5 % [v/v] β-mercaptoethanol, 1 % [w/v] bromophenol blue) and boiled for 5 min. Using the standard modifications of the described protocol (Laemmli, 1970), equal amounts of total protein were loaded and separated by SDS-PAGE using a 12 % (v/v) resolving gel (1.5 M Tris-HCl, pH 8.8) and a 4 % (v/v) stacking gel (0.5 M Tris-HCl, pH 6.8). The gels were electrophoresed for 1.5 hours at 120 V in 1x SDS running buffer (25 mM Tris-HCl pH 8.3, 192 mM glycine, 0.1 % [w/v] SDS). The Blue Prestained

molecular weight ladder (Thermo Scientific) was used in order to estimate the molecular weights of the resolved proteins. Once the SDS-PAGE gels were run, Western blot analysis was performed on the proteins according to the established protocol (Towbin, Staehelin, & Gordon, 1979). The separated proteins on the SDS-PAGE gel were transferred onto a nitrocellulose membrane for 50 min at 0.4 A using Western transfer buffer (13 mM Tris-HCl, 100 mM glycine, 20% [v/v] methanol). Confirmation of the protein transfer from the gel to the membrane was carried out using Ponceau staining (0.5 % [w/v] Ponceau S, 1 % [v/v] glacial acetic acid). The membranes were blocked using 1 % BLOTTO (1 % [w/v] BLOTTO in Tris buffered saline [1x TBS, 50 mM Tris, 150 mM NaCl, pH 7.5]) for 1 hour. The membranes were incubated with primary antibody (mouse anti-HA tag antibody 1:1000 dilution, Abcam Cat #: AB9110) at 4 °C overnight in 1 % BLOTTO and then washed with TBS-Tween-20 (TBS-T: 0.1 % [v/v] Tween®-20 in TBS) for 4 x 5 minute washes. The membranes were incubated with Donkey Anti-Rabbit IgG H&L (Horseradish peroxidase (HRP), 1:10000 dilution, Abcam Cat #: AB16284) secondary antibody for 30 minutes at 22 °C in 1 % BLOTTO and then washed with TBS-T for 4 x 5 minute washes. Detection of proteins was carried out using an enhanced chemiluminescence (ECL) substrate together with the ChemiDocTM XRS+ System (Bio-Rad, USA).

Fluorescent CYP3A4 activity assay

The activity assay used was a modification of the methods used by Oscarson et al. (2002) and Murayama et al. (2001). The conversion of the synthesized 7-benxyloxy-4-trifluoromethylcoumarin (50 µM) was determined in reaction mixtures containing 0.1 M potassium phosphate pH 7.4, cell lysate corresponding to 1 mg of total protein, and 50 µM 7-benzyloxy-4-trifluoromethylcoumarin in a total volume of 100 µl. The reactions were initiated by addition of NADPH to a final concentration of 1 mM and the mixture incubated for 45 min at 37 °C with end-over-end rotation at 6 rpm. The reaction was stopped by addition of 10 µl 0.3 M perchloric acid followed by the addition of 10 µl 1 M NaOH. The samples were centrifuged at 1500 x *g* for 10 min and the supernatant was transferred to a black walled 96-well plate. The amount of 7-hydroxy-4-trifluoromethylcoumarin (Renwick et al., 2001) was measured using fluorescence (Ex410:Em538). The amount of 7-hydroxy-4-trifluoromethylcoumarin detected at this wavelength was measured as the activity of the enzymes.

Cell proliferation assay

Cell proliferation of the transfected HEK293-CYP3A4-HA, HEK293-pcDNA3.1+ and untransfected HEK293 cell lines was tested using a cell counting assay. Cells were seeded at a density of 1 x 10^5 cells/ml into 24-well plates (12 wells per cell line, 3 wells per time point: 24 hrs; 48 hrs; 72 hrs and 96 hrs) and incubated for 24 hours at 37 °C at 9 % CO_2. At each time point the cells were lifted using trypsin and live cells counted using trypan blue (1:1 ratio with cells) and a hemocytometer coupled to Zeiss phase contrast light microscope. All cells were counted a minimum of three times at 24, 48, 72 and 96 hour time points and the cell growth between cell lines was compared over time.

This assay was also used to assess the viability of the HEK293-CYP3A4-HA, HEK293-pcDNA3.1+ and untransfected HEK293 cell lines after treatment with propranolol or labetalol. Cells were seeded at 0.5 x 10^5 cells/ml in a 24-well plate, incubated overnight at 37 °C, 9 % CO_2 and treated with either 50 µM propranolol or 50 µM labetalol. An untreated sample was assessed as a control. Cells were counted at 48 and 72 hrs. At each time point the cells were lifted using trypsin and counted using trypan blue (1:1 ratio with cells) and a hemocytometer on a Zeiss phase contrast light microscope. All cells were counted a minimum of three times and the cell growth between cell lines was compared over time.

Colorimetric cell viability assay

The effect of the compounds on cell survival and proliferation in the HEK293-CYP3A4-HA and HEK293-pcDNA3.1+ cell lines was determined using the MTT assay according to the manufacturer's instructions. Cells were seeded at a density of 1 x 10^5 cells/ml into 96-well plates and incubated overnight at 37 °C, 9 % CO_2. The cells were treated with varying concentrations of each compound and incubated for 72 hours at 37 °C, 9 % CO_2. After 72 hours all liquid was removed from the wells and 50 µL of MTT (1 in 5 dilution) cell proliferation reagent (Sigma-Aldrich) was added to each well of the plates and incubated at 37 °C for 4 hours. A total of 100 µL of solubilisation solution (10 % [w/v] SDS, 0.01 M HCl) was added to each well and incubated at 37 °C overnight. Cell density was determined by absorbance measured at 595 nm using a microtitre plate reader (Spectromax). The experiment was carried out in triplicate on each of the plates.

High performance liquid chromatography (HPLC) assessment of CYP3A4 metabolites

The HPLC system used for analysis and chromatographic separation consisted of a UFLC/UFLC$_{XR}$ Shimadzu Model CBM-20A Prominence bus modulator, a Model LC-20AB Prominence liquid chromatograph, a Model SIL-20A Prominence auto sampler and a Model RF-20A Prominence fluorescence detector. LabSolutions Version 5.71 was used as the data acquisition software. Analysis was performed on a Luna 5 µm C_{18} (2) 100 Å column with an internal diameter of 150 x 4.6 mm. A SecurityGuard™ cartridge C18 4 x 3.0 mm was attached to the column prior to analysis. All chemicals were weighed using a Radwag AS 220/C/2 analytical balance 220 g x 0.1 mg. On a daily basis and prior to analysis solutions were agitated in order to produce homogenous samples using a Scientific Industries Model G-560E Vortex Genie-2 mixer. The mobile phase used comprised of 35:65:0.1 acetonitrile, 0.05 M sodium dihydrogen orthophosphate dihydrate and triethylamine, respectively. The mobile phase was adjusted to pH 3 with a Mettler Toledo SevenEasy pH meter using 2 M ortho-phosphoric acid. The buffer was filtered using a 0.45 µm HV Millipor Durapor® Membrane filter and degassed under vacuum using a Spellbound® Laboratory Solutions Dry Vac 801 vacuum pump. Standard stock solutions of propranolol (1 mg/ml) were prepared and transferred into 1.5 ml brown screw chromatographic, HPLC autosampler headspace vials which were used for all samples. The stock solutions were made up in the mobile phase to the desired maximum concentration and then serial dilution to produce the desired range of concentrations.

In order to investigate the metabolism of propranolol using HPLC, the protocol for the CYP3A4 activity assay was followed with modifications. A reaction mixture containing 0.1 M potassium phosphate pH 7.4, cell lysate corresponding to 1 mg of protein and 16 µg/ml propranolol in a total volume of 500 µl was prepared. The reactions were initiated by adding NADPH to a final concentration of 1 mM and left for 48 hours at 37 °C with end-over-end rotation at 6 rpm. Two control samples were also prepared; one without NADPH and the other without lysate. After 48 hours the reaction was quenched by adding 50 µl 0.3 M perchloric acid followed by 50 µl 1 M NaOH. Following quenching, the samples were centrifuged at 1500 x *g* for 10 min. Solid phase extraction of these analytes was done using Oasis HLB 3 cc (60 mg) extraction cartridges and a Preppy 12-port vacuum manifold. The cartridges were conditioned with 1 ml acetonitrile and subsequently equilibrated with 1 ml water. The analytes were loaded onto the cartridges and collected in glass vials. The cartridges were washed with 500 µl water and these samples

were also collected in glass vials. For the final wash, 500 µl acetonitrile was used and these samples were collected in glass vials. The acetonitrile solution was used for analysis using HPLC. The samples were transferred into 1.5 ml brown screw chromatographic, HPLC autosampler headspace vials and sodium dihydrogen orthophosphate buffer was added to the sample in the desired volume to achieve the same proportions as that of the mobile phase. All samples were agitated with a vortex prior to analysis.

Reproducibility and Statistical analysis

Unless otherwise stated, all assays were conducted in triplicate. Statistical analysis was carried out in GraphPad Prism 4.03 software (GraphPad Inc., 2005).

CHAPTER 3 RESULTS

3.1 In silico profiling of metabolism in comparison to results reported by literature.

Rational for determination of known compounds for use in metabolic studies

Propranolol, labetalol, rosiglitazone and chlorpromazine have been reported to be CYP3A4 substrates, resulting in the production of toxic metabolites in cell-based studies (Rana, Will, Nadanaciva, & Jones, 2016) (Gustafsson, Foster, Sarda, Bridgland-Taylor, & Kenna, 2014). In addition to CYP3A4, propranolol and labetalol are also known to be metabolized by CYP2D6 to form toxic metabolites (Narimatsu et al., 1997) (Danielson, 2002). Rosiglitazone has also, alternatively, been shown to be mainly metabolized by CYP2C8 and also CYP2C9 (in a small capacity) (Baldwin, Clarke, & Chenery, 2001) and chlorpromazine has been associated with CYP2B1 metabolism (Baldwin et al., 2001).

Propranolol **(Figure 3A**) has been reported to undergo oxidative metabolism via hydroxylation of the naphthalene ring at either the 4, 5 or 7 position as well as *N*-desisopropylation (Masubuchi et al., 1994) (**Scheme 4**). Labetalol (**Figure 3B**) is mainly metabolised through conjugation from its glucuronide, however, it has been reported that the compound also undergoes *N*-dealkylation which results in 3-amino-1-phenyl butane (Rurak et al., 1992) (Gal, Zirrolli, & Lichtenstein, 1988) and is further oxidized into either benzylacetone and 3-amino-1-(4-hydroxyphenyl)butane (**Scheme 5**). However, this metabolic pathway is not completely understood and the metabolism of labetalol is relatively unclear (Rurak et al., 1992). Rosiglitazone (**Figure 3C**) is extensively metabolized with the main routes being identified as *N*-demethylation and pyridine ring hydroxylation (Baldwin et al., 2001) (**Scheme 6**). For chlorpromazine (**Figure 3D**), the main established metabolic pathway is *N*-oxidation (Boehme & Strobel, 1998). Another study has revealed the presence of other metabolites, namely: 7-hydroxy, a sulfoxide, an *N*-desmethyl and an *N*-desmethylsulfoxide (Hawes et al., 1991) (**Scheme 7**).

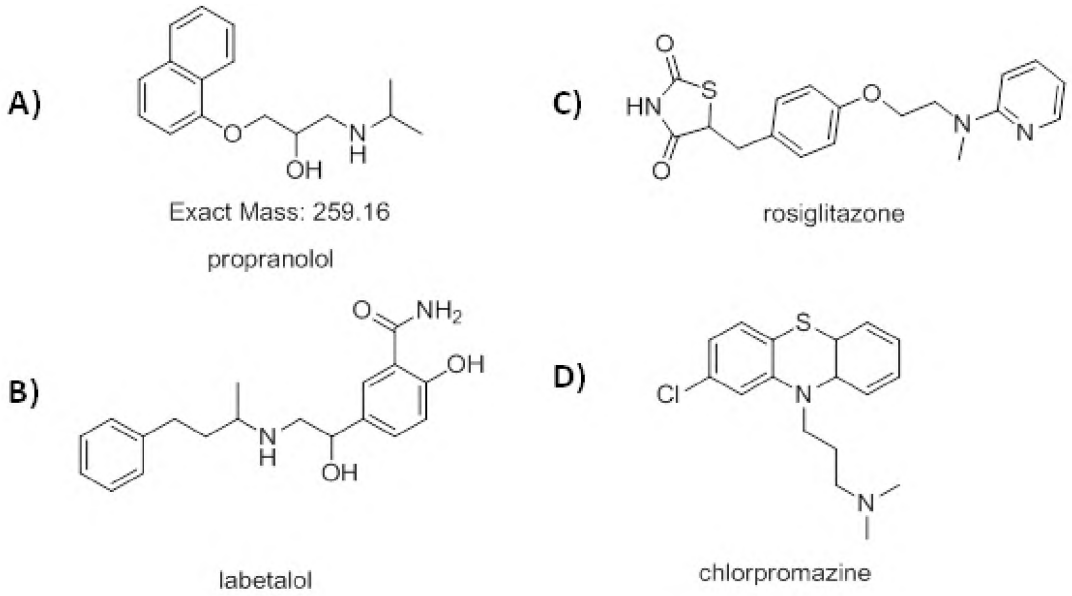

Figure 3: Structures of propranolol, labetalol, rosiglitazone and chlorpromazine. *Structure of* ***(A)*** *propranolol,* ***(B)*** *labetalol,* ***(C)*** *rosiglitazone and* ***(D)*** *chlorpromazine the known CYP3A4 substrates to be used in metabolism studies and their exact masses.*

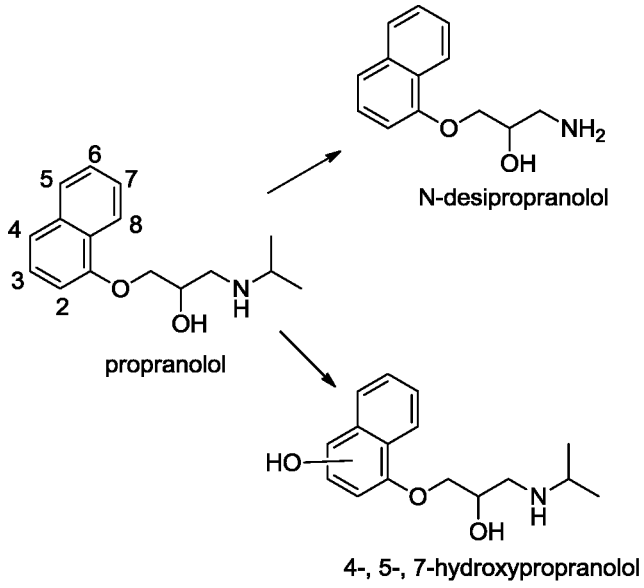

Scheme 4: Metabolism of propranolol. *Metabolic pathway of propranolol and the resulting main metabolites as proposed by Masubuchi et al. (2000). This metabolism results in 4-, 5-, or 7-hydroxypropranolol and N-desipropranolol.*

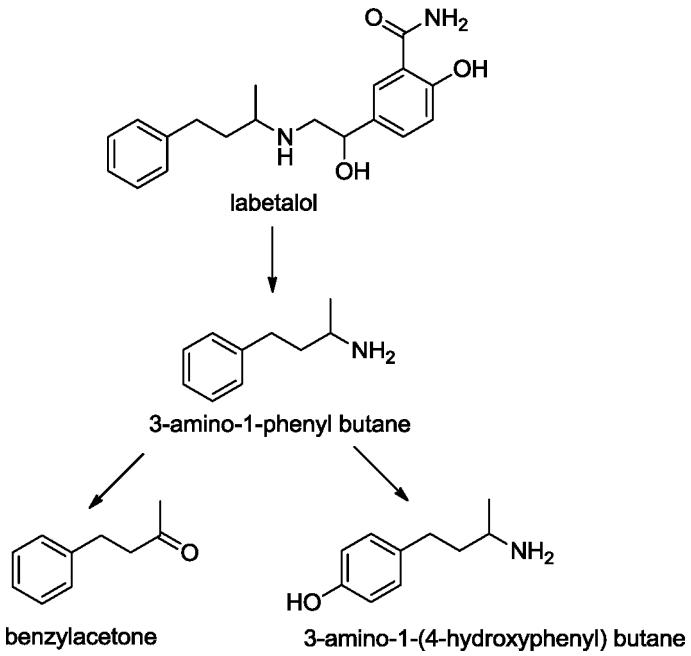

Scheme 5: Metabolism of labetalol*. Metabolic pathway of labetalol as proposed by Rurak et al. (1992) which results in the main metabolite 3-amino-1-phenyl butane and further oxidation into either benzylacetone or 3-amino-1-(4-hydroxyphenyl) butane.*

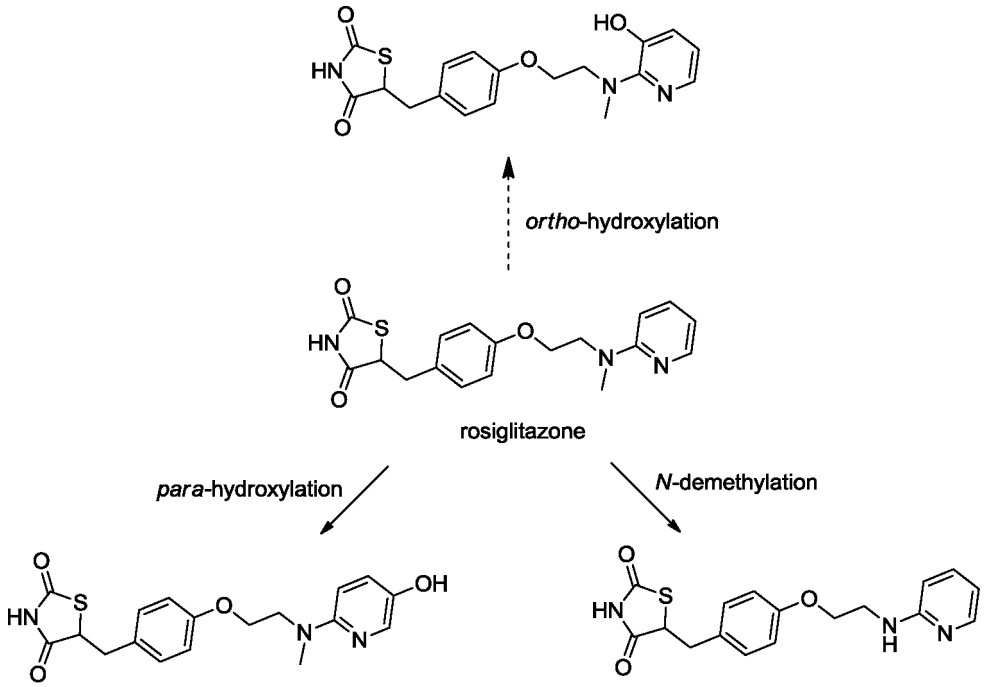

Scheme 6: Metabolism of rosiglitazone*. Metabolic pathway of rosiglitazone and the resulting metabolites as proposed by Baldwin et al. (2001). The metabolites result due to either hydroxylation or N-demethylation. Major pathways are indicated by solid arrows and the minor pathway is indicated by a broken arrow.*

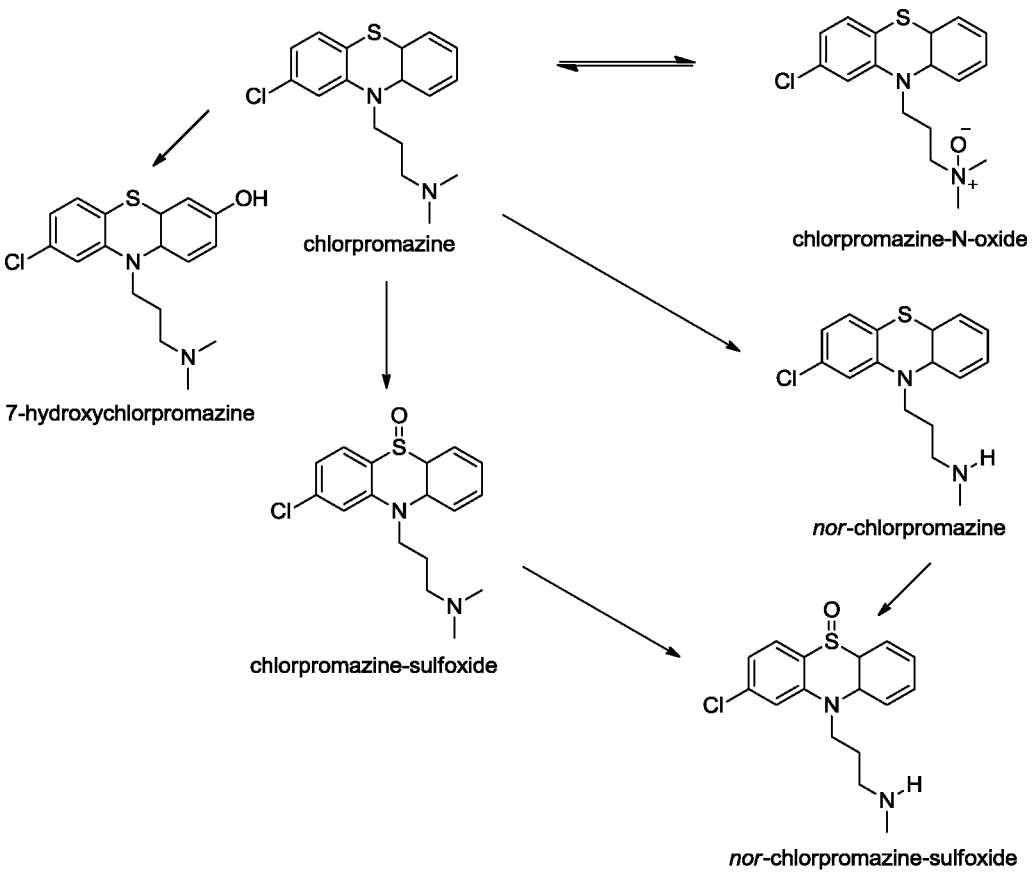

Scheme 7: Metabolism of chlorpromazine*. Metabolic pathway of chlorpromazine and resulting metabolites as proposed by Hawes et al. (1991). The main metabolite being chlorpromazine-N-oxide and the other resulting metabolites are 7-hydroxychlorpromazine, chlorpromazine-sulfoxide, nor-chlorpromazine and nor-chlorpromazine sulfoxide (which is metabolized from chlorpromazine-sulfoxide or nor-chlorpromazine).*

We were interested in subjecting our compounds to *in silico* analysis, for the purposes of comparing the results to our *in vitro* data and published data. Our first test was to subject propranolol, labetalol, rosiglitazone and chlorpromazine to analysis by pkCSM (predicting small-molecule pharmacokinetic and toxicity properties using graph-based signatures), a freeware program. This resource predicts a number of ADME properties using graph-based signatures (Pires et al., 2015). pkCSM has the added advantage in that it is machine learning which relies upon learning patterns between similarity, chemical composition, pharmacokinetic and toxicity properties to be able to predict drug models, this is better because the "discovering implicit patterns consistent and valid for unseen data" (Pires et al., 2015). It provides a very rapid and simple method to evaluate compounds during the early stages of drug development (Pires et al., 2015). Importantly for our purposes, pkCSM predicts whether a particular compound is a likely substrate for CYP2D6 or CYP3A4. In addition, it predicts whether the compound in question will inhibit several other CYP450 enzymes.

We were specifically interested in identifying if any of the compounds would be predicted as substrates for CYP3A4. In accordance with several studies, propranolol, rosiglitazone and chlorpromazine were predicted to be CYP3A4 substrates, (**Figure 8A, C** and **D**) while labetalol was not (**Figure 8B**). **Figure 8B** does however, highlight that labetalol is a substrate for CYP2D6 which is in accordance with the study by Danielson (2002). According to this prediction, chlorpromazine is also a substrate for CYP2D6 (**Figure 8D**). In addition, this software also predicts labetalol to be an inhibitor of CYP2D6 (**Figure 8B**) and also predicts the same for propranolol (**Figure 8A**) and chlorpromazine (**Figure 8D**).

It is possible for a compound to be both a substrate for and an inhibitor of a specific CYP450 enzyme as was predicted for labetalol with regards to CYP2D6 (**Figure 8B**). Lynch & Price (2007) reported that erythromycin, both inhibits and is metabolized by CYP3A4 (Ray et al., 2004). Further investigation into literature yielded evidence that labetalol inhibits CYP2D6 (Lacey, Armstrong, & Goldman, 2007).

A)

Molecule Depiction

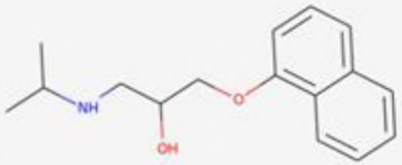

SMILES

Property	Model Name	Predicted Value	Unit
Metabolism	CYP2D6 substrate	No	Categorical (Yes/No)
Metabolism	CYP3A4 substrate	Yes	Categorical (Yes/No)
Metabolism	CYP1A2 inhibition	Yes	Categorical (Yes/No)
Metabolism	CYP2C19 inhibition	No	Categorical (Yes/No)
Metabolism	CYP2C9 inhibition	No	Categorical (Yes/No)
Metabolism	CYP2D6 inhibition	Yes	Categorical (Yes/No)
Metabolism	CYP3A4 inhibition	No	Categorical (Yes/No)

B)

Molecule Depiction

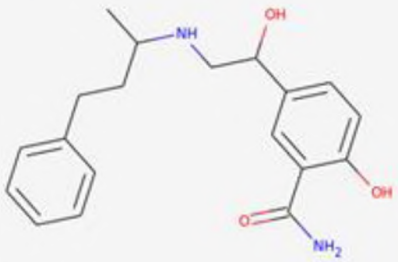

SMILES

Property	Model Name	Predicted Value	Unit
Metabolism	CYP2D6 substrate	Yes	Categorical (Yes/No)
Metabolism	CYP3A4 substrate	No	Categorical (Yes/No)
Metabolism	CYP1A2 inhibition	No	Categorical (Yes/No)
Metabolism	CYP2C19 inhibition	No	Categorical (Yes/No)
Metabolism	CYP2C9 inhibition	No	Categorical (Yes/No)
Metabolism	CYP2D6 inhibition	Yes	Categorical (Yes/No)
Metabolism	CYP3A4 inhibition	No	Categorical (Yes/No)

C)

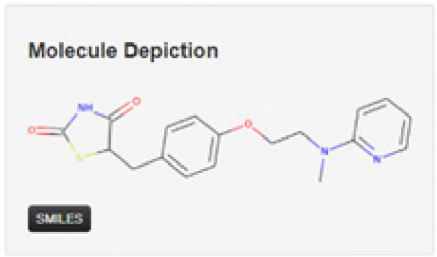

Property	Model Name	Predicted Value	Unit
Metabolism	CYP2D6 substrate	No	Categorical (Yes/No)
Metabolism	CYP3A4 substrate	Yes	Categorical (Yes/No)
Metabolism	CYP1A2 inhibitior	Yes	Categorical (Yes/No)
Metabolism	CYP2C19 inhibitior	Yes	Categorical (Yes/No)
Metabolism	CYP2C9 inhibitior	No	Categorical (Yes/No)
Metabolism	CYP2D6 inhibitior	No	Categorical (Yes/No)
Metabolism	CYP3A4 inhibitior	No	Categorical (Yes/No)

D)

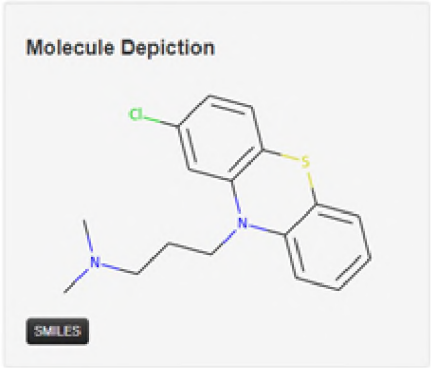

Property	Model Name	Predicted Value	Unit
Metabolism	CYP2D6 substrate	Yes	Categorical (Yes/No)
Metabolism	CYP3A4 substrate	Yes	Categorical (Yes/No)
Metabolism	CYP1A2 inhibitior	Yes	Categorical (Yes/No)
Metabolism	CYP2C19 inhibitior	No	Categorical (Yes/No)
Metabolism	CYP2C9 inhibitior	No	Categorical (Yes/No)
Metabolism	CYP2D6 inhibitior	Yes	Categorical (Yes/No)
Metabolism	CYP3A4 inhibitior	No	Categorical (Yes/No)

Figure 8: pkCSM predictions of labetalol, propranolol, rosiglitazone and chlorpromazine. *The software program pkCSM was utilized to predict which CYP450 isoforms would metabolize* ***(A)*** *propranolol,* ***(B)*** *labetalol,* ***(C)*** *rosiglitazone and* ***(D)*** *chlorpromazine. This program also predicted which compounds inhibit certain CYP450 isoforms.*

The other *in silico* prediction software used, ChemAxon JChem Metabolizer (Pirok, 2013), is able to predict the major metabolites of substrates by making use of a biotransformation library which contains generic metabolism reactions. This software is also able to predict the percentage likelihood of each metabolite resulting from metabolism and with most substrates it can also predict the unlikely metabolites (Pirok, 2013). This software is useful in that it can be used to aid *in vitro* metabolism studies by establishing preliminary metabolism data.

The main metabolites predicted for propranolol are both as a result of metabolic dealkylation (Youdim & Riederer, 2004) which results in the formation of a free amine or hydroxy and a corresponding aldehyde or ketone, depending on the degree of substitution (**Figure 9**, Metabolite 1 and 2). Metabolite 1, *N*-desipropranolol, (**Scheme 4**) was identified as a major metabolite in the literature, and was predicted as having a 84.34 % likelihood of forming from metabolism, (**Figure 9** Metabolite 1). 4-Hydroxypropranolol (Metabolite 5) which has also identified as a major metabolite from CYP450 oxidation in the literature (**Scheme 4**) was predicted as 'unlikely' with only a 0.018 % chance of occurring (**Figure 9**, Metabolite 5).

In silico predictions for labetalol suggested that the three main metabolites each had a 28.38 % likelihood of occurring (**Figure 10**). This prediction shares a degree of similarity to the scheme proposed by Rurak et al. (1992) (**Scheme 5**) with the exception of the position of hydroxylation on Metabolite 1.

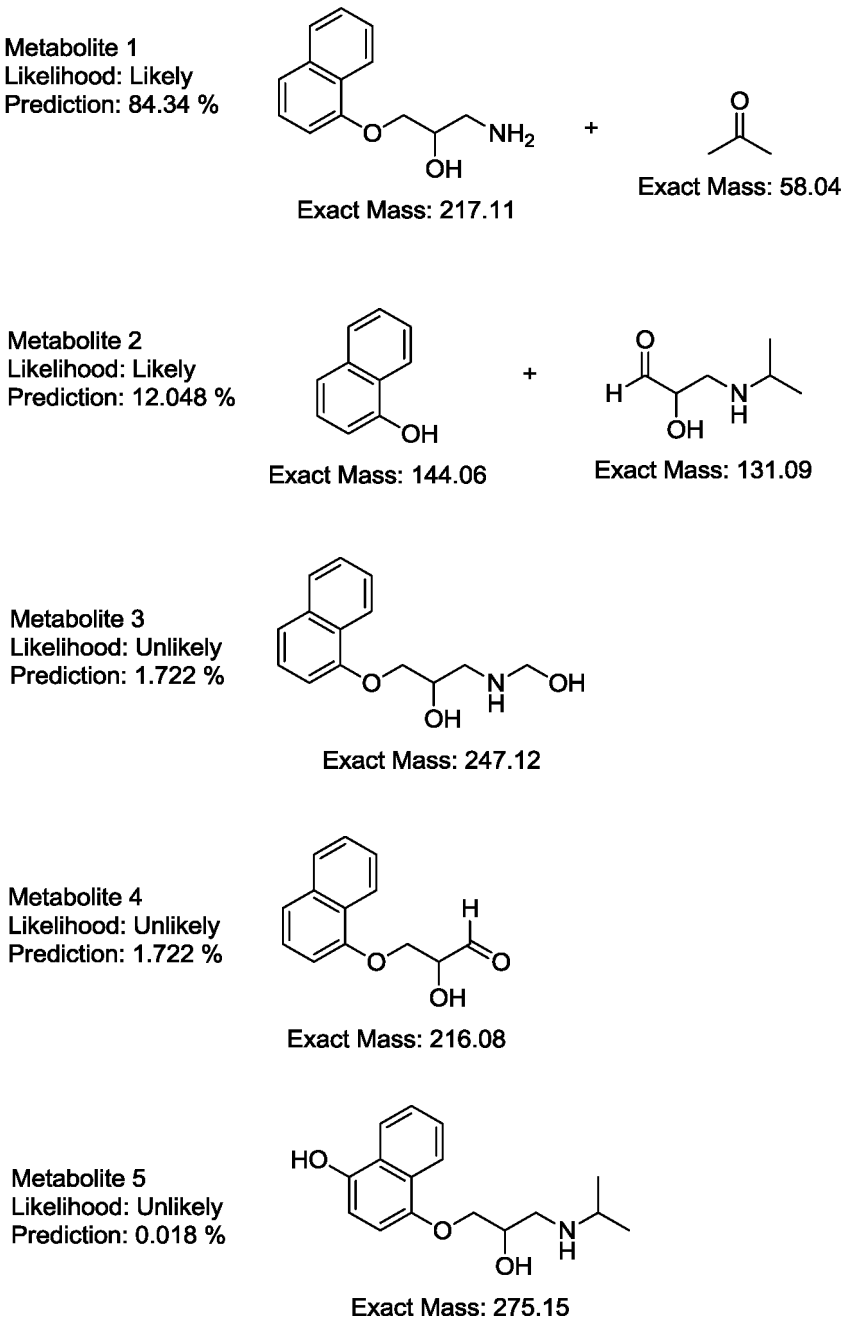

Figure 9: Propranolol metabolite prediction. *Prediction of the five main metabolites which results from propranolol metabolism. The likelihood of each compound and prediction (%) is also included. Predictions were done using the ChemAxon JChem Metabolizer software.*

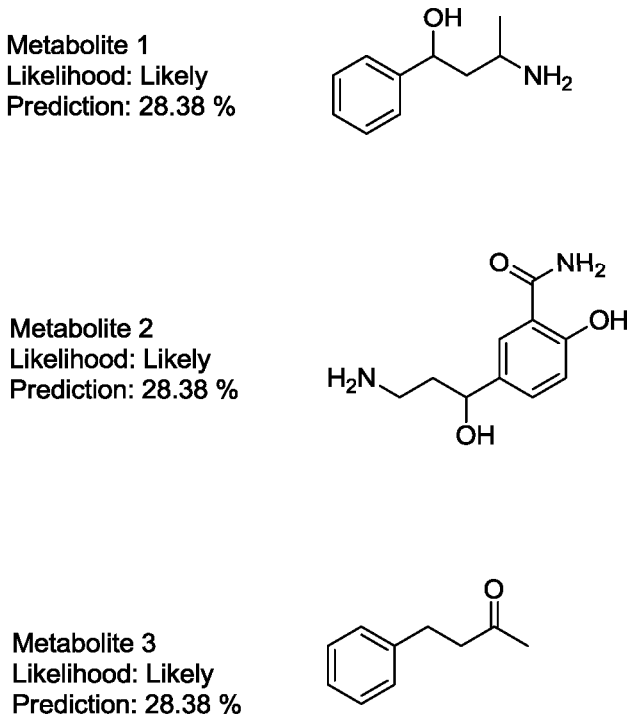

Figure 10: Labetalol metabolite prediction. *Prediction of the three main metabolites which results from labetalol metabolism. The likelihood of each compound and prediction (%) is also included. Predictions were done using the ChemAxon JChem Metabolizer software.*

In terms of rosiglitazone, four main metabolites were predicted with this software with the main metabolite having a 56.6 % probability of occurring (**Figure 11**, Metabolite 1) and the other three metabolites all having an 8.1 % chance of being produced (**Figure 11**). From all four predicted metabolites, only Metabolite 4 had previously been reported by literature (**Scheme 4**) (Baldwin et al., 2001). This prediction bares a small resemblance to the scheme proposed by Baldwin et al. (2001) in which the metabolite resulting from *N*-demethylation is a major metabolite, whereas, in the prediction in **Figure 11** this metabolite only has a 8.1 % chance of occurring (**Figure 11**, Metabolite 4).

The metabolizing software for chlorpromazine predicted three metabolites. The main metabolite has a 75.6 % likelihood of occurring (**Figure 12**, Metabolite 1), the second metabolite is predicted to have a 10.8 % chance of occurring and the last metabolite only having a 1.56 % chance. When compared to literature (**Scheme 5**), all three predicted metabolites were proposed to be main chlorpromazine metabolites (Hawes et al., 1991). Even though Hawes et al. (1991) proposed the formation of metabolites other than chlorpromazine-sulfoxide, *nor*-chlorpromazine and chlorpromazine-*N*-oxide

(which is the main metabolite proposed by (Hawes et al., 1991)) this prediction closely resembles that of **Scheme 5** (Hawes et al., 1991).

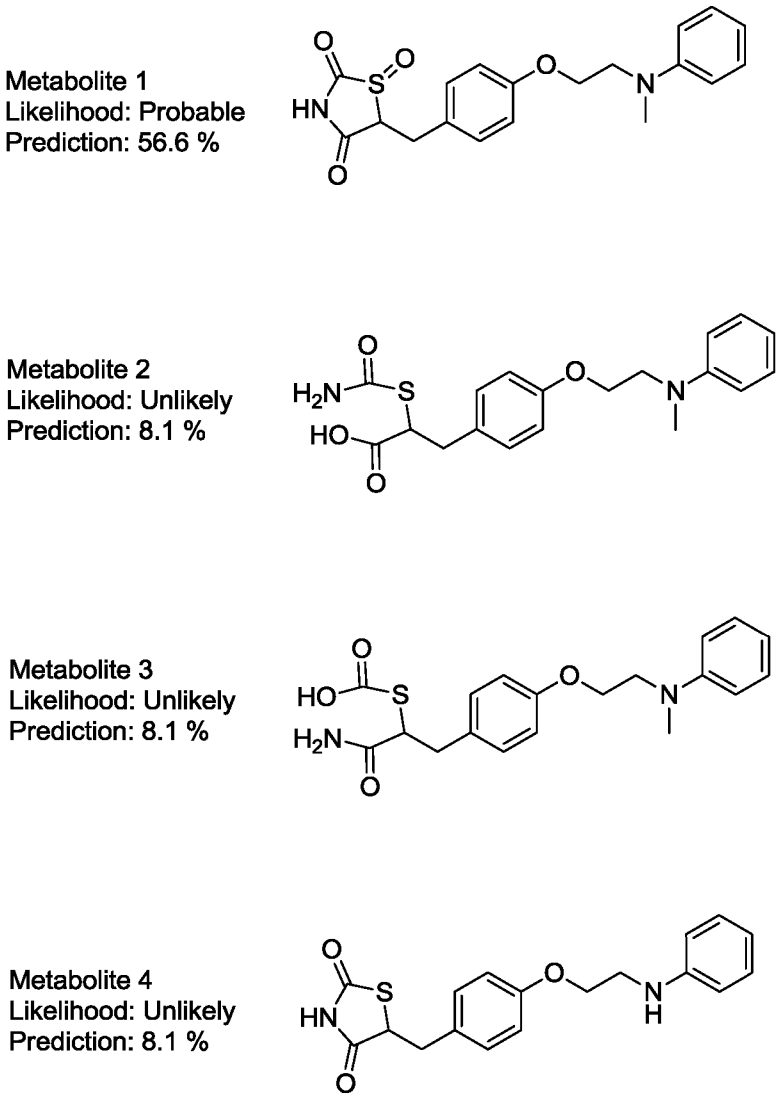

Figure 11: Rosiglitazone metabolite prediction*. Prediction of the 4 main metabolites which results from rosiglitazone metabolism. The likelihood/probability of each compound and prediction (%) is also included. Predictions were done using the ChemAxon JChem Metabolizer software.*

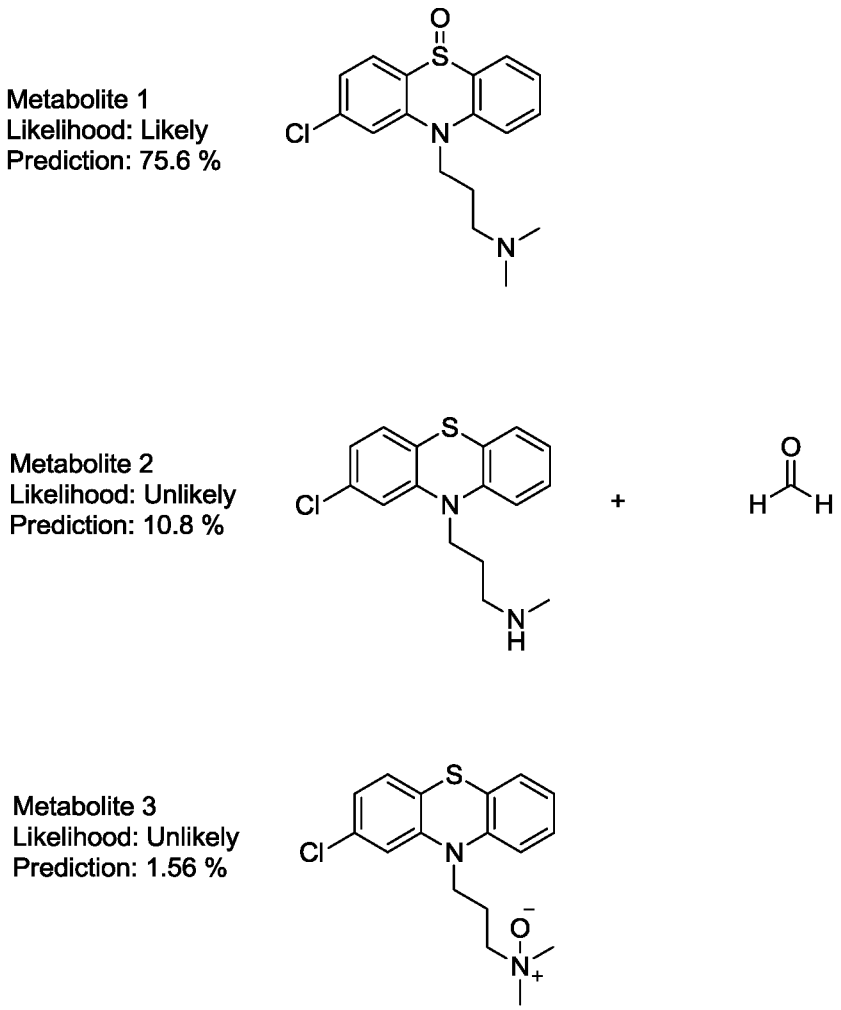

Figure 12: Chlorpromazine metabolite prediction*. Prediction of the three main metabolites which results from chlorpromazine metabolism. The likelihood of each compound and prediction (%) is also included. Predictions were done using the ChemAxon JChem Metabolizer software.*

To summarise, *in silico* prediction using pkCSM suggests that only propranolol, rosiglitazone and chlorpromazine are substrates for CYP3A4 (**Figure 8**), while prediction of the major metabolites of all the compounds suggest that metabolic dealkylation is the major path of metabolism, which is only partially represented in the literature.

3.2 Creation and validation of HEK293 cell line stably expressing CYP3A4 (and the equivalent control).

CYP3A4 plasmid design, transfection and proof of concept

Part of the aim of this study was to develop a stable cell line which overexpressed CYP3A4. Our goal with this was first to develop a platform from which we could assess possible metabolic toxicity of any compounds tested against this line as per the approach of Gustafsson et al. (2014). Furthermore, we could use these cell lysates as an *in vitro* comparison for *in silico* predictions. For these purposes, we designed an appropriate plasmid for expression of CYP3A4 in a mammalian cell line. This plasmid was transfected into HEK293 cells using standard protocols resulting in the creation of a stable cell line. **Figure 13** shows the structure of the pcDNA3.1+/CYP3A4 plasmid used for expression of CYP3A4 in mammalian cell lines. This plasmid vector was designed with an in frame HA (Human influenza hemagglutinin) tag for identification of the CYP3A4-HA protein using Western blotting analysis. In addition, the plasmid contained resistance vectors to certain antibiotics, which is required for selection of the CYP3A4-HA plasmid in both bacterial and mammalian cell lines (**Figure 13**). **Figure 13A** also displays the presence of two unique restriction enzyme sites present on either side of the CYP3A4 insert, *Nhe*I and *Xho*I. These enzymes were used to validate the identity of the plasmid by performing a restriction digestion analysis. Due to the enzymes being placed in specific areas it is possible to predict where in the plasmid the cut will occur and the sizes of the corresponding linear DNA fragments.

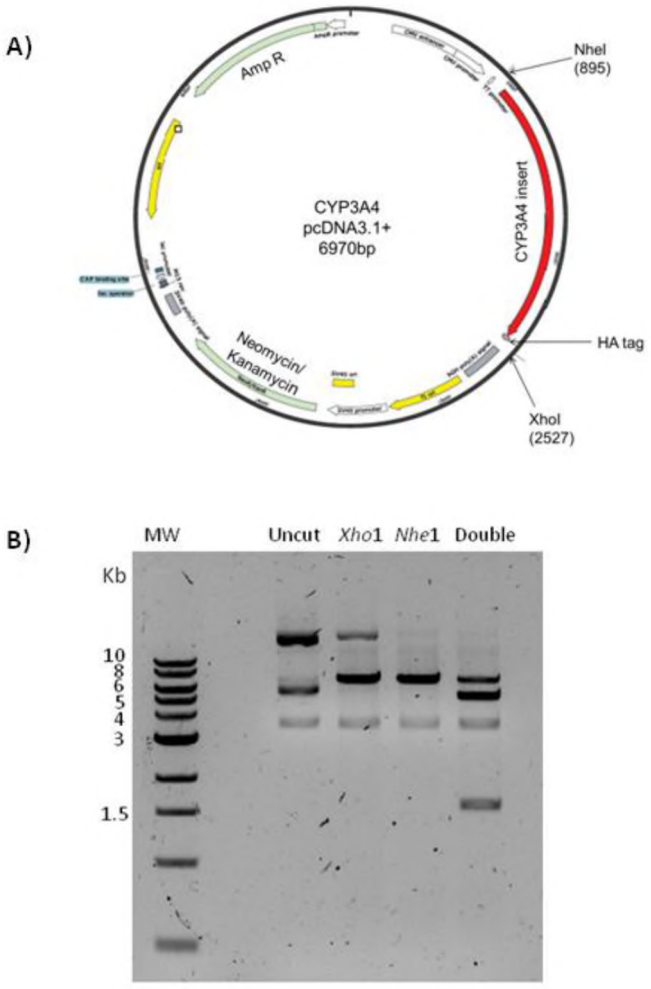

***Figure 13: Plasmid map and restriction digest**. **A)** pcDNA3.1+ backbone plasmid which was designed with a CYP3A4 insert using SnapGene software. **B)** Validation of pcDNA3.1+ CYP3A4-HA plasmid by restriction digestion analysis using 1% agarose gel.*

The restriction digestion was analysed by agarose gel electrophoresis as shown in **Figure 13B**. The different bands in the uncut lane represents three different conformations of the uncut circular plasmid DNA, which is to be expected. The *Xho*1 lane displays an additional visible band of a lower mobility, which is partially uncut DNA and corresponds to one of the DNA conformations in the uncut lane. The linearized DNA in the *Xho*1 lane is displayed at approximately 7000 bp which is the approximate size of the pcDNA3.1+/CYP3A4-HA plasmid which is calculated as 6970 bp (**Figure 13A**). The *Nhe*1 lane also displays the linearized DNA at approximately 7000 bp which is, again, the predicted size of the linearized plasmid. The first band in the double cut lane (which combines both *Nhe*1 and *Xho*1 enzyme treatment) corresponds to the pcDNA3.1+ backbone (~5500 bp) and the second band represents the CYP3A4-HA

insert (~1500 bp). This validates the presence of the pcDNA3.1+/CYP3A4-HA plasmid (**Figure 13B**). Following this validation, the plasmid was transfected into HEK293 cells.

Following transfection, the cells were transferred into new medium containing the selection antibiotic G418. This resulted in the death of cells which had not taken up the plasmid and were therefore not resistant to G418. This selection process resulted in the presence of cells which, theoretically, contained the CYP3A4-HA plasmid or the pcDNA3.1+ backbone for the control cell line. **Figure 14A** and **B** exhibits the growth of the stable cell lines over a period of nine weeks. The formation of colonies could be observed in both cell lines, two weeks after transfection. After five weeks, colonies big enough to be seen with the naked eye could be observed with both cell lines, however, more colonies were present in the HEK293-CYP3A4-HA transfected cell line. The colonies were subsequently transferred from 10 cm dishes into T25 flasks to aid expansion. It was also noted that the HEK293-CYP3A4-HA cell line appeared to be growing at an increased rate compared to the HEK293-pcDNA3.1+ cell line (**Figure 14A** and **B**). Western blot analysis confirmed the expression of the CYP3A4-HA protein in the transfected cell line but not the control (**Figure 14C**).

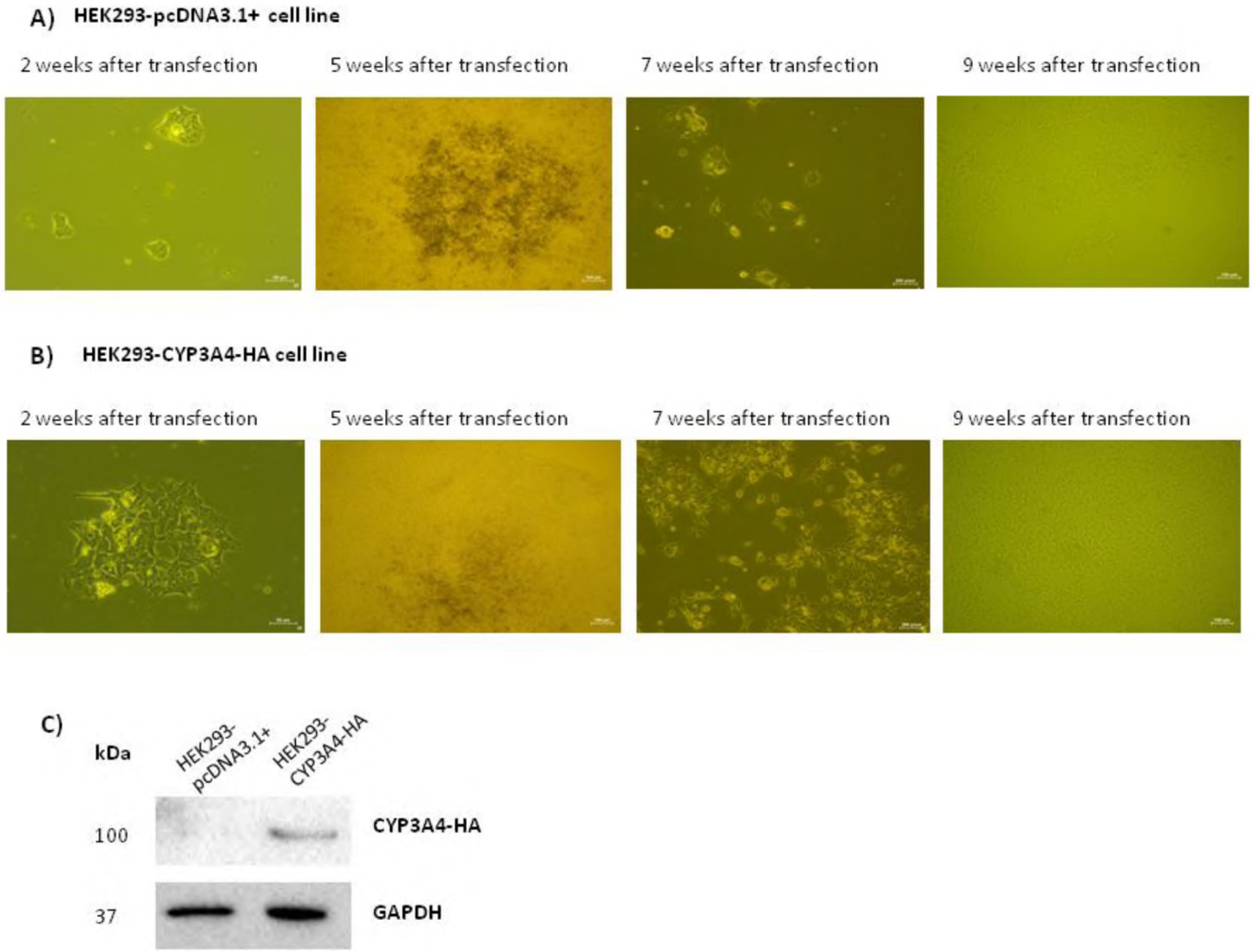

***Figure 14: Generation of HEK293 cell line stably expressing CYP3A4-HA. A** and **B)** HEK293 cells transfected with either pcDNA3.1+ or pcDNA3.1+/CYP3A4-HA at various weeks after transfection and during selection. **C)** Western blot analysis confirming the presence of the CYP3A4-HA protein in the HEK293-CYP3A4-HA cell line and absence in the HEK293-pcDNA3.1+ cell line. GAPDH was used as a loading control.*

Analysis of the proliferation rates of the transfected cell lines compared to an untransfected HEK293 cell line

Observations during generation of the cell lines suggested that the HEK293-pcDNA3.1+ and HEK293-CYP3A4-HA cell lines proliferated at different rates. In order to test this, a cell proliferation assay was performed using the untransfected HEK293 cell line as a control. The HEK293-CYP3A4-HA cell line exhibited an increased proliferation rate compared to the HEK293-pcDNA3.1+ and untransfected HEK293 cell lines (**Figure 15**). In addition, the HEK293-pcDNA3.1+ and untransfected HEK293 cell lines had similar proliferation rates (**Figure 15**). These data suggested that the transfected CYP3A4 enzyme might give the HEK293 cells a proliferative advantage. Another theory is that the use of the polyclonal culture system method could have reduced the proliferation of the HEK293-pcDNA3.1+ cell line due to the same construct being taken up in different areas of the cell in the different clones.

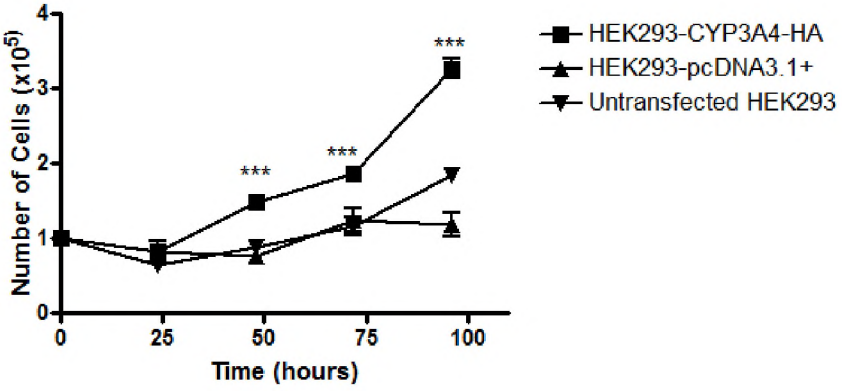

Figure 15: HEK293-CYP3A4-HA cell lines grow faster than control cell lines. *Graph displaying the change in cell number over time as determined by cell counting assay with an untransfected HEK293 cell line and HEK293-CYP3A4-HA and HEK293-pcDNA3.1+ transfected cell lines. This assay was performed in triplicate and read at different time points (24 hrs, 48 hrs, 72 hrs and 96 hrs) in triplicate. Error bars indicate standard deviation (n=3). Statistical significance was calculated using a two way ANOVA Bonferroni posttests with a P value of < 0.001 indicated by ***.*

Synthesis of 7-benzyloxy-4-trifluoromethyl-coumarin a CYP3A4 substrate

Having successfully generated the HEK293-CYP3A4-HA cell line, our next step was to confirm the enzymatic activity of the overexpressed CYP3A4-HA enzyme *in vitro*. The compound 7-benzyloxy-4-trifluoromethyl-coumarin is routinely used in the pharmaceutical industry to screen new chemical entities as potential inhibitors of CYP3A4 (Wang et al., 1997). This substrate is metabolized into 7-hydroxy-4-trifluoromethyl-coumarin by CYP3A4 which exhibits a diagnostic excitation wavelength of 410 nm and fluorescent emission at 538 nm (Code et al., 1997) (Sridar et al., 2008). Accordingly, we tested the activity of the CYP3A4 enzymes being expressed in our transformed cell using this marker substrate. Owing to the high cost of this substrate, we undertook a modified two-step synthetic procedure of 7-benzyloxy-4-triflouromethyl-coumarin (DeGrote et al., 2014) (Tyndall et al., 2015).

The Pechmann condensation is a common method used for the synthesis of coumarin derivatives which involves the condensation of a phenol with a β-ketoester, under mildly acidic conditions (DeGrote et al., 2014). Wu, Diao, Sun, & Li (2006) were able to improve the yield and selectivity of this synthesis through the incorporation of molecular iodine as a catalyst. In addition, they found that non-polar solvents, such as toluene, favour the Pechmann condensation and result in higher yields when added in small amounts (<1 ml). Using the optimized conditions as outline by DeGrote et al. (2014) a percentage yield of 45 % was obtained following flash chromatography (**Scheme 16**).

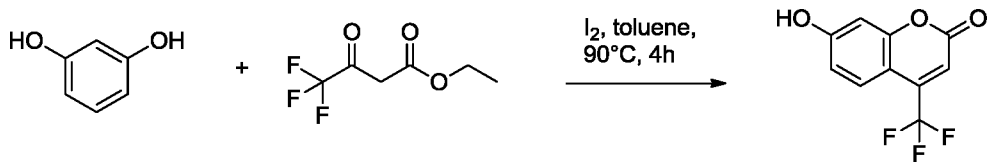

Scheme 16: Reaction scheme of intermediate, 7-hydroxy-4-(trifluoromethyl) 2H-chromen-2-on. *Synthesis of 7-hydroxy-4-(trifluoromethyl) 2H-chromen-2-one with resorcinol and ethyl-4,4,4-trifluoroacetoacetate catalyzed by iodine and using toluene as a solvent as proposed by DeGrote et al. (2014). Reaction was kept at a constant temperature of 90 °C for 4 hours.*

The final step of the reaction involved benzylation of the phenol group of 7-hydroxy-4-(trifluoromethyl) 2H-chromen-2-one, with benzyl bromide and potassium carbonate in acetonitrile (**Figure 17**). The method for this synthesis was modified from Keglevich et al. (2008).

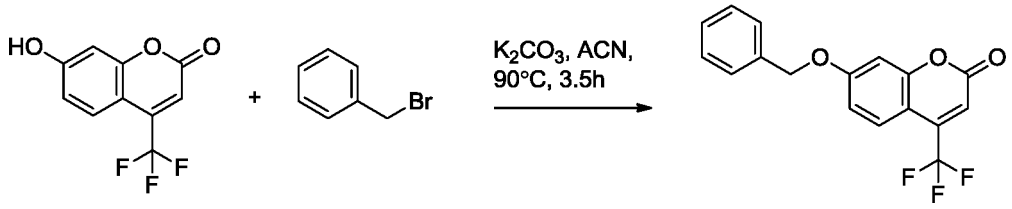

Scheme 17: Reaction scheme of final product, 7-benzyloxy-4-trifluoromethyl-coumarin*. Synthesis of 7-benzyloxy-4-trifluoromethyl-coumarin with 7-hydroxy-4-(trifluoromethyl) 2H-chromen-2-one and benzyl bromide, addition of potassium carbonate and using acetonitrile as a solvent as adapted from Keglevich et al. (2008) . Reaction was kept at a constant temperature of 90 °C for 3 and a half hours.*

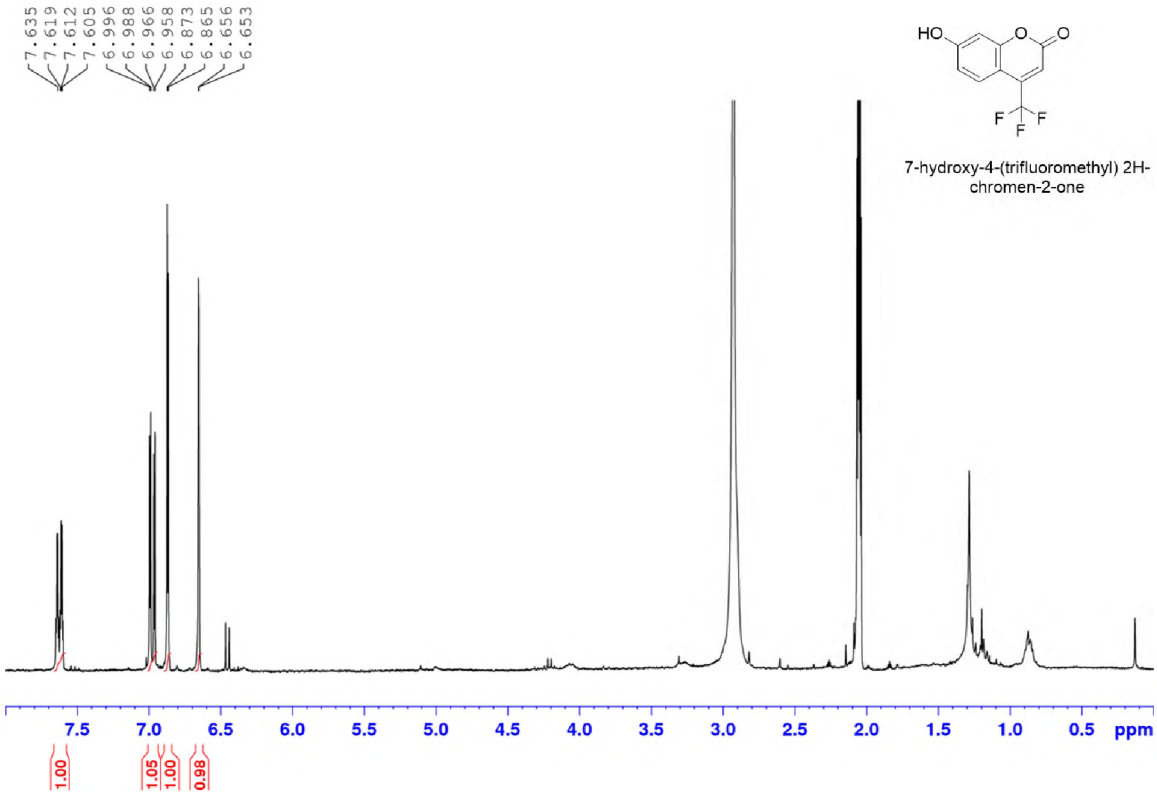

Figure 18: **1H NMR spectrum (300 MHz, Acetone-D_6) for 7-hydroxy-4-(trifluoromethyl) 2H-chromen-2-one.**

The synthesis of the intermediate (7-hydroxy-4-(triflouromethyl) 2H-chromen-2-one) and final product (7-benzyloxy-4-triflouromethyl-coumarin) was validated with NMR analysis which is depicted in **Figure 18 and in Figure 19**.

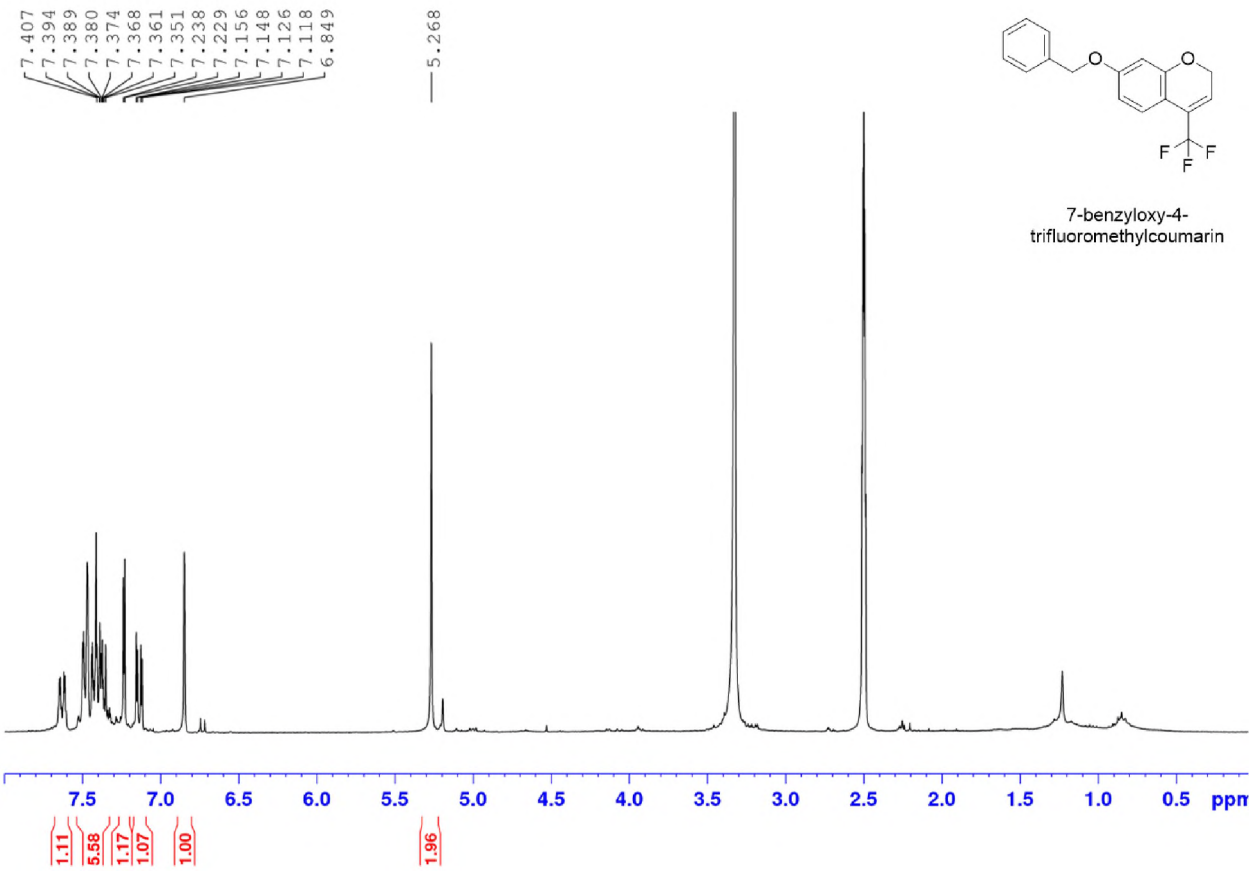

Figure 19: **1H NMR spectrum (300 MHz, DMSO-D_6) for 7-benzyloxy-4-triflouromethyl-coumarin.**

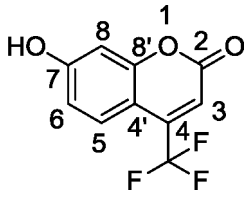

7-hydroxy-4-(trifluoromethyl) 2H-chromen-2-one

7-hydroxy-4-(trifluoromethyl) 2H-chromen-2-one (1), 45 % yield, White solid; ^{1}H NMR (Acetone, 300 MHz) δH 7.51 - 7.48 (1H, dd, *J* = 9.0, 2.5 Hz, H-5), 6.87 - 6.83 (1H, dd, *J* = 9.0, 2.5 Hz, H-6), 6.74 (1H, d, *J* = 2.5 Hz, H-8), 6.53 (1H, s, H-3) ppm.

The spectrum for 7-hydroxy-4-(trifluoromethyl) 2H-chromen-2-one (**1**) corresponds to that reported by Xie et al. (2015).

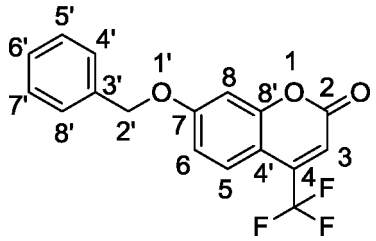

7-(benzyloxy)-4-(triflouromethyl) 2H-chromen-2-one

7-Benzyloxy-4-trifluoromethylcoumarin (2), 90 % yield , White solid; ^{1}H NMR (DMSO, 300 MHz) δ_H 7.65 - 7.61 (1H, dd, *J* = 9.0, 2.5 Hz, H-5), 7.50 - 7.35 (6H, m, H-3'-8'), 7.24 - 7.23 (1H, d, *J* = 2.5 Hz, H-8), 7.16 - 7.12 (1H, dd, J = 9.0, 2.5 Hz, H-6), 6.85 (1H, s, H-3), 5.27 (2H, s, H-2') ppm.

The experimental data (**2**) for 7-benzyloxy-4-trifluoromethylcoumarin corresponds to that of DeGrote et al. (2014).

Based on these data, we concluded that we had successfully synthesised the CYP3A4 substrate.

Establishing CYP3A4 enzyme activity

Making use of the synthesized CYP3A4 substrate, 7-benzyloxy-4-trifluoromethyl-coumarin, we optimized the activity assay based on the methods by Oscarson et al. (2002) and Murayama et al. (2001) to determine the CYP3A4 enzyme activity in our cell lysates (**Figure 20**).

The first activity assay was adapted from Oscarson et al. (2002) and Murayama et al. (2001). However, there was no significant difference in fluorescence activity between the CYP3A4 transfected lysates and the untransfected HEK293 lysates when using the published assay. Therefore, it was necessary to optimise the assay for our conditions. Varying certain experimental conditions such as substrate concentration (50 µM), buffer system (potassium phosphate buffer), NADPH (0.1 mM), incubation time (45 minutes) and total measured protein in the lysate (1 mg) (data not shown) optimized the activity assay in order to prove CYP3A4 activity in the pcDNA3.1+/CYP3A4-HA transfected cell line (**Figure 20**). All the data in **Figure 20** were subtracted from the untransfected HEK293 samples in order to exhibit activity of the CYP3A4. A statistically significant difference ($P < 0.0011$) was found between the other samples and the pcDNA3.1+/CYP3A4-HA cells at 1 mg total protein exhibiting CYP3A4 activity.

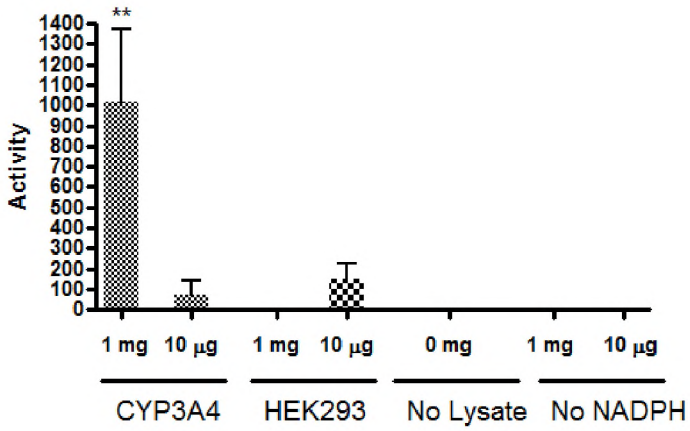

Figure 20: CYP3A4 activity assay. *Graph showing metabolic activity of the HEK293-CYP3A4-HA cell lysates compared to untransfected HEK293 cells and two controls (no lysate and no NADPH) at varying substrate concentrations and times. The activity assay was done in triplicate. The activity assay was performed under the following experimental conditions: incubation for 45 min 37 °C; 0.1 M potassium phosphate pH 7.4 buffer system; 50 µM substrate concentration; 1 mg or 10 µg protein from cell lysates; 0.1 mM NADPH; the mixture was pre-warmed at 37 °C and the protein was added last. Error bars indicate standard deviation (n=3). Statistical significance was calculated using a one way ANOVA Bonferroni posttests with with a P value of < 0.0011 indicated by **. All samples were read at Ex 410: Em 538. All samples were subtracted from the untransfected HEK293 cell samples.*

3.3 Metabolism studies of known compounds.

Cytotoxicity Testing

Rana et al. (2016) have previously utilised a Hep3 hepatoma cell line to overexpress metabolic cytochrome enzymes, for the purposes of assaying compounds for metabolic toxicity (Rana et al., 2016). In their study, propranolol and labetalol were both identified as substrates of CYP3A4, whose metabolism resulted in cytotoxicity. Labetalol was implicated in a similar study using HepG2 cells (Hosomi et al., 2011). Furthermore, rosiglitazone and chlorpromazine were identified as producing cytotoxic metabolites following CYP3A4 oxidation in a similar study using T-antigen immortalised human liver epithelial cells (Gustafsson et al., 2014).

Having confirmed that our cell lines were producing active CYP3A4 (**Figure 20**), we resolved to utilise the four abovementioned compounds shown to be metabolised by CYP3A4 to determine whether we could observe metabolic induced cytotoxicity. All four compounds were used in cell viability assays against the CYP3A4-expressing and control cell line (**Figure 21**). As can be seen in **Figure 21**, chlorpromazine had an

IC_{50} of 16.59 µM in the HEK293-CYP3A4-HA cell line and an IC_{50} value of 19.45 µM in the HEK293-pcDNA3.1+ cell line. Rosiglitazone had an IC_{50} value of 100.1 µM in the HEK293-CYP3A4-HA cell line and a value of 97.98 µM in the HEK293-pcDNA3.1+ control cell line. This shows a statistically insignificant difference between IC_{50} values in the both the cell lines when the same concentration of a compound is used. In the HEK293-CYP3A4-HA cell line propranolol had an IC_{50} value of 84.32 µM and 93.30 µM in the control cell line, while labetalol values were 73.19 µM and 93.98 µM in the HEK293-CYP3A4-HA and HEK293-pcDNA3.1+ cell lines, respectively.

These results indicated that there was no significant difference in the IC_{50} values in either the CYP3A4 expressing or control cell line for any of the four compounds tested (**Figure 21**). Whilst unexpected, the lack of differences in toxicity between the two cell lines in the presence of these four compounds is an interesting result and leads to some important questions being asked. Are these compounds actually substrates for CYP3A4? Are the CYP3A4 metabolites the cause of the toxicity observed by Gustafsson et al. (2014) and Rana et al. (2016)? Is their reported metabolic induced toxicity a result of background metabolism stemming from the use of liver cells? Is the lack of differential cytotoxicity in our study as a result of enhanced cellular proliferation of the CYP3A4 cell line? And finally, does this result call into question the validity of extrapolating complex metabolic toxicity data from a cell-based assay?

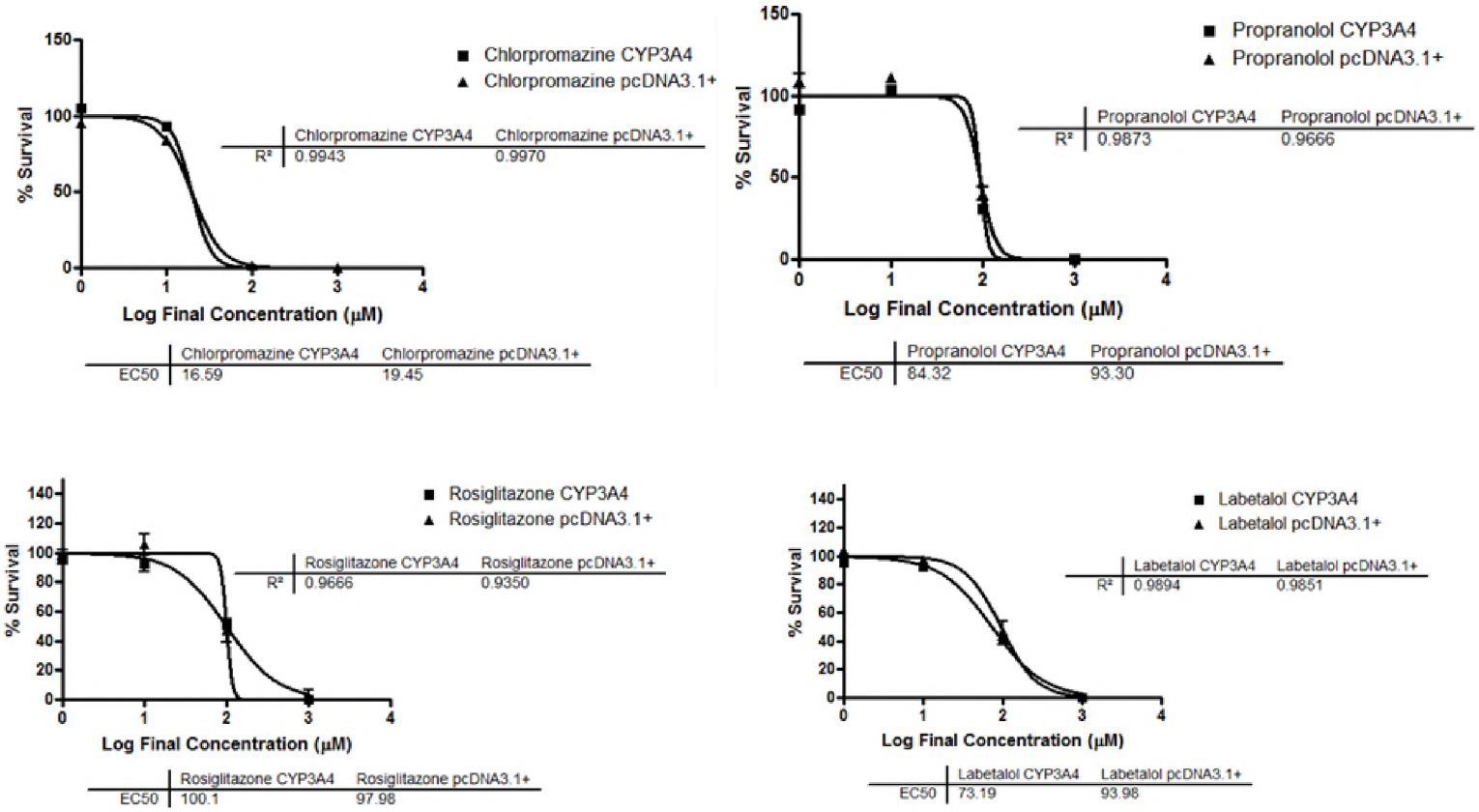

Figure 21: Cell viability assay of compounds. MTT cytotoxicity assay of rosiglitazone, chlorpromazine, propranolol and labetalol in the HEK293-CYP3A4-HA and the control HEK293-pcDNA3.1+ cell lines. All assays were performed in triplicate at each concentration. The cells were treated with a range of concentrations (1000 µM, 100 µM, 10 µM, 1 µM, 0.1 µM). IC_{50} values were calculated by non-linear regression using GraphPad 4.0 and were determined separately from each data set.. Equation used: Y=Bottom + (Top-Bottom)/(1+10^((LogEC50-X)*HillSlope)). X is the logarithm of concentration. Y is the response.

Cytotoxicity Cell Counting Assay

In light of the results obtained from the colorimetric MTT inhibition studies (**Figure 21**), we hypothesised that the increased growth rate of the HEK293-CYP3A4-HA cell line (**Figure 15**) may have influenced the results of the MTT assay. We therefore assessed the effect that propanolol and labetolol would have over time in a cell counting assay. Propranolol and labetalol reduced cell viability in the HEK293-CYP3A4-HA cell line when compared to an untreated control, which is statistically significant ($P < 0.0001$) and can be seen in **Figure 22A**.

However, propranolol and labetalol did not decrease cell viability in the HEK293-CYP3A4 cell line compared to either the HEK293-pcDNA3.1+ or the untransfected HEK293 cell line. In fact, the stably transfected HEK293-pcDNA3.1+ cells appeared to be more sensitive to both labetalol and propranolol than the other two cell lines (**Figure 22B** and **C**). This decrease in cell viability was statistically significant ($P < 0.01$) when compared to HEK293-CYP3A4-HA when treated with propranolol and labetalol. This could potentially be attributed to the decreased proliferative rate of this cell line which has previously been exhibited in **Figure 15**. Conversely, the decreased sensitivity of the HEK293-CYP3A4-HA cell line to propranolol and labetalol (**Figure 22B** and **C**) could be as a result of the increased proliferative rate of this stably transfected cell line which was shown earlier in the cell counting assay (**Figure 15**).

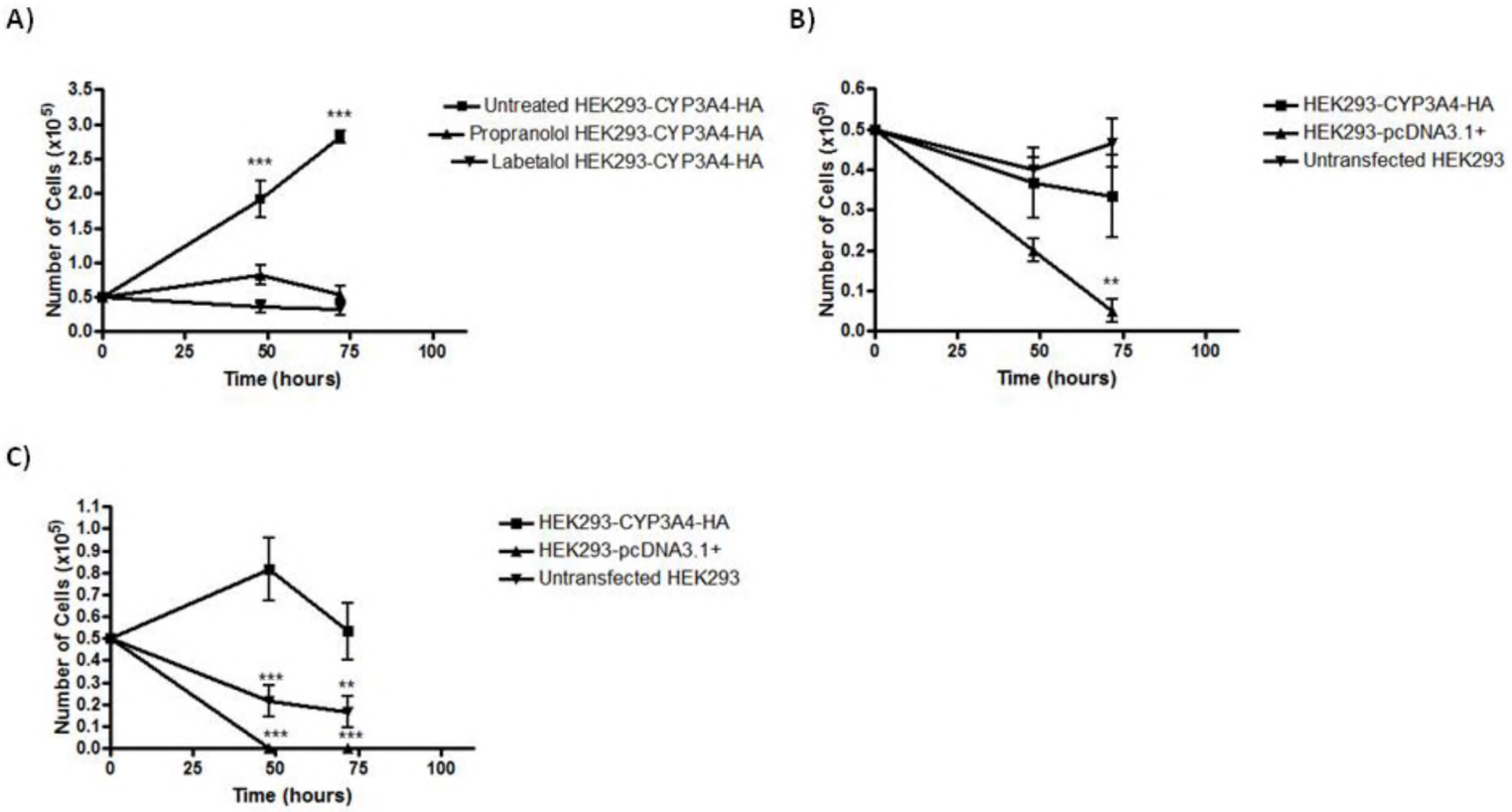

Figure 22: Cytotoxicity cell counting in known compounds*. This assay was performed in triplicate using the transfected HEK293-CYP3A4-HA, HEK293-pcDNA3.1+ and untransfected HEK293 cell lines and read at different time points (48 hrs and 72 hrs) in triplicate.* ***A)*** *Graph displaying cytotoxicity cell counting in HEK293-CYP3A4-HA cell line of untreated and labetalol and propranolol treated cells for comparative purposes. Error bars indicate standard deviation (n=3). Statistical significance was calculated using a two way ANOVA Bonferroni posttests with a P value of < 0.0001 indicated by ***.* ***B)*** *Graph displaying cytotoxicity cell counting assay in HEK293-CYP3A4-HA, HEK293-pcDNA3.1+ and untransfected HEK293 cell lines after being treated with 50 µM labetalol. Statistical significance was calculated using a two way ANOVA Bonferroni posttests with a P value of < 0.01 indicated by **.* ***C)*** *Graph displaying cytotoxicity cell counting assay in HEK293-CYP3A4-HA, HEK293-pcDNA 3.1+ and untransfected HEK293 cell lines after being treated with 50 µM propranolol. Statistical significance was calculated using a two way ANOVA Bonferroni posttests with a P value of < 0.01 indicated by ** and a P value of < 0.001 indicated by ***. Error bars indicate standard deviation (n=3).*

Taken together, the results of both the MTT and cell counting cytotoxicity assays indicated that the CYP3A4 expressing cell line was not more sensitive to the compounds than the control cell lines.

High-performance liquid chromatography to test metabolism using CYP3A4 enriched lysates

Despite showing that our CYP3A4 enzyme was active, we were not able to observe any toxicity with the putative CYP3A4 substrate compounds. We therefore attempted to confirm that these compounds were being metabolised by the CYP3A4 enzyme using HPLC methods. For this study, we used propranolol as the standard compound.

Optimization of HPLC Method

In order to detect metabolites by HPLC we first needed to develop and optimise the method. This included selecting the appropriate stationary and mobile phase, detection system and validation of the reproducibility of the assay.

Stationary phase (column) selection

In order to select the analytical column literature was consulted and in particular a paper by Botterblom, Feenstra, & Erdtsieck-Ernste (1993) in which a C_{18} reverse phase 250 x 4.6 mm I.D. was used for the HPLC analysis of propranolol and labetalol. The choice of column/stationary phase is the first crucial step in method development (Bhavani & Durga, 2015) and as such a high performance column must be used in order to obtain robust and reproducible results. Reverse phase C_{18} are commonly used columns as they provide exceptional peak shape and can also be used over a wide pH range (2-9 (Agilent Technologies, 2006)). In addition these columns are non-polar and as a result shorten the retention times for more hydrophobic compounds (Snyder, Kirkland, & Glajch, 1997). Based on the better retention time, good column life as well as easy availability the Luna® 5 µm C_{18} (2) 100 Å column with an internal diameter of 150 x 4.6 mm was selected as a suitable column for HPLC analysis.

Mobile phase selection

Mobile phase selection is an important parameter to consider in method development as it can have major impacts on the retention as well as selectivity of compounds (Haddad, Drouen, Billiet, & De Galan, 1983). The selection of the mobile phase for this analysis was based on the work done by Botterblom et al. (1993) in which they used 35:65:0.1 (v/v) acetonitrile, 0.05 M sodium dihydrogen orthophosphate dihydrate and triethylamine, respectively to detect propranolol. In addition, it is well suited for high sensitivity analysis which makes use of short wavelengths and has a higher elution strength (Shimadzu, 2017a). Triethylamine is added in order to avoid peak tailing (Botterblom et al., 1993) and also results in better separation of peaks (Gheshlaghi, Scharer, Moo-Young, & Douglas, 2008). The sodium dihydrogen orthophosphate is merely added to the mobile phase to act as a buffer system. An increase or decrease in the pH of the mobile phase can have an impact on the retention time of compounds. It is known that ionisation occurs when pH < pK_a and because any ionized molecules are significantly retained, the retention time of compounds will increase when pH is decreased to below 3.7 (Dolan, Snyder, & Kirkland, 2013).

The first mobile phase attempted for this analysis was a mixture of 35:65 acetonitrile and water, respectively, however adequate peak separation was not achieved and the retention time for propranolol was significantly decreased (**Figure 23A**). The mobile phase consisting of 35:65:0.1 (v/v) acetonitrile, orthophosphate sodium dihydrogen dihydrate and triethylamine (Botterblom et al., 1993) resulted in adequate separation of the peak, increased the retention time of propranolol and even appeared to increase the sensitivity of the analysis (**Figure 23B**).

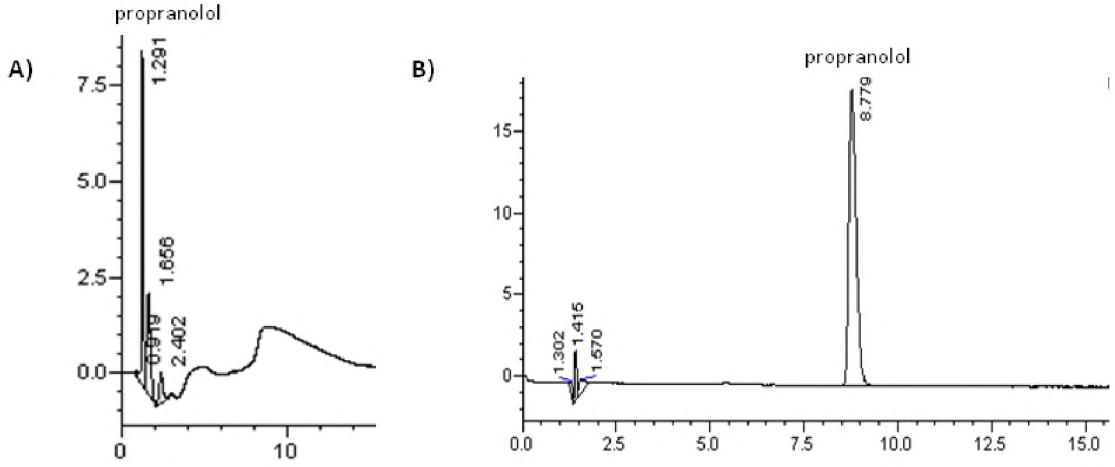

Figure 23: Optimization of HPLC mobile phase system. A) *Chromatograph of propranolol at a concentration of 100 µg/ml utilizing a mobile phase system of 35:65 acetonitrile and water. The unit of measurement is mAU at wavelength 254 nm.* ***B)*** *Chromatograph of propranolol at a concentration of 100 µg/ml utilizing a mobile phase system of 35:65:0.1 (v/v) acetonitrile, sodium dihydrogen orthophosphate dihydrate and triethylamine The unit of measurement is mAU at wavelength 254 nm.*

Method of detection

The detector of the HPLC is responsible for producing a measurable signal which corresponds to a specified concentration. The choice of the chromatographic detector should be based on precision, selectivity, sensitivity and linear dynamic range (Swartz, 2010). Ultraviolet (UV) detection is most commonly used and makes use of either a variable wavelength or photo diode-array detector (PDA). This method of detection is considered to be fairly sensitive with extremely broad linearity (Swartz, 2010). However, when tested with our samples this method of detection proved to be insufficient in detecting the compound (**Figure 24**). According to literature, fluorescence (FL) detection "may provide the selectivity and sensitivity necessary for routine analysis of plasma propranolol concentrations" (Hedeen, Tyczkowska, Aucoin, & Norton, 1991). Hedeen et al. (1991) reported that the detection limit of propranolol using a fluorescence detector was 1 ng/ml and the linear regressions for the standard curves (2.5-100 ng/ml) gave correlation coefficients which were above 0.9955. Fluorescence detectors have also been shown to be as much as 100 times more sensitive than UV detectors. This characteristic is useful with analysis of low concentration samples (Swartz, 2010). As a result, this method of detection appeared promising and therefore propranolol was detected using the fluorescence at a 230 nm excitation wavelength and a 340 nm emission wavelength (Kim, Hong, Park, Kang, & Lee, 2001), which increased the sensitivity of our measurements as can be seen from the numbers presented on the y-axis

(**Figure 24B**). As can be noted in **Figure 24** the two propranolol peaks in **Figure 24A** and **B** have different retention times which is due to the analyses being performed on two separate days resulting in varying environmental temperatures.

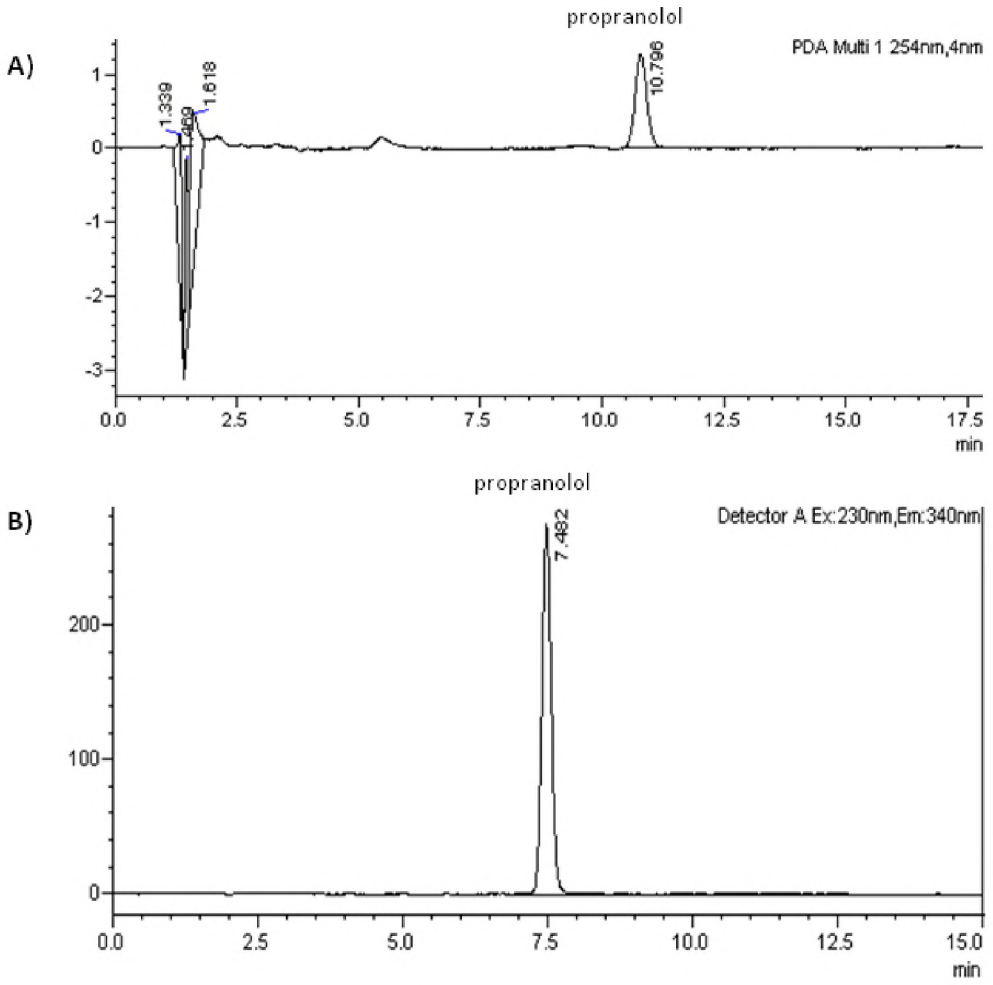

Figure 24: Optimization of HPLC method of detection. A) *Chromatogram of propranolol at a concentration of 1 µg/ml using a photodiode array detector (PDA) at wavelength 254 nm. The unit of measurement is mAU.* ***B)*** *Chromatograph of propranolol at a concentration of 1.25 µg/ml using a fluorescence detector. The unit of measurement is mV, Ex: 230 nm, Em: 340 nm.*

In addition to increased sensitivity, the fluorescence detector also exhibited better linearity at a lower concentration compared with the PDA detector (**Figure 25**). Calibration standard solutions were injected in ascending order of concentration and a calibration curve of peak area (mAU or mV) vs concentration (µg/ml) was plotted and is shown in **Figure 25**. The correlation coefficient for propranolol with the PDA detector was 0.8832 in the range 10-100 µg/ml (**Figure 25A**), whereas with the FL detector, the correlation coefficient was 0.9057 for propranolol in the range 0.313-10 µg/ml (**Figure 25B**). These results indicated that the FL detector was the optimal method of detection for propranolol. However, in

order to draw an accurate conclusion from this graph, we would need to include the same number of points for both curves.

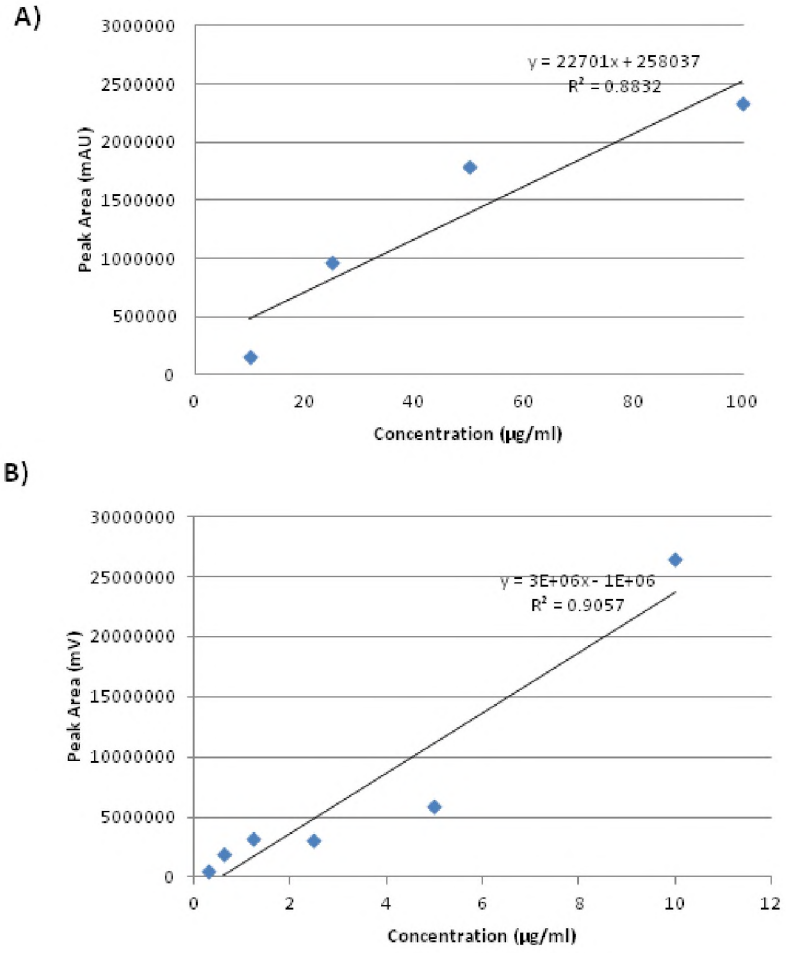

Figure 25: Propranolol standard curves using different methods of detection. A) *Standard curve for propranolol measuring peak area over the concentration range 10-100 µg/ml using a PDA detector.* ***B)*** *Standard curve for propranolol measuring peak area over the concentration range 0.313-10 µg/ml using a FL detector.*

Optimization of reproducibility

Another aspect of the HPLC analysis which needed to be optimized was the reproducibility between runs of the same sample. Initially, we noticed that there was a large disparity in retention time between consecutive runs of the same sample, which we attributed to inappropriate sample solvent (Shimadzu, 2017b) (data not shown). An article by Agilent (2013) mentioned that the sample solvent has to be compatible with the HPLC mobile phase as well as the HPLC column used. Therefore, it was decided to change the solvent in which the sample was dissolved. Previously, all samples were dissolved in a

mixture of 35:65 acetonitrile and water, respectively. As a result, the sample solvent was changed to that of the mobile phase (35:65:0.1 [v/v] acetonitrile, 0.05 M sodium dihydrogen orthophosphate dihydrate and triethylamine). This change resulted in better reproducibility between samples.

Metabolism Studies and Solid Phase Extraction

Once the method of detection for propranolol had been optimized the next step was to perform the metabolism studies and solid phase extraction in order to prepare the samples for analysis utilizing HPLC. **Figure 26** highlights the optimized method developed for the metabolism of propranolol (retention time 3.6 min) and detection of possible metabolites formed. Various cell lysates and controls were used in order to confirm the presence of any metabolites only in the HEK293-CYP3A4-HA lysates. In **Figure 26A** a small peak was detected at 1.5 min from the HEK293-CYP3A4-HA lysates, which we suspected could be a polar propranolol metabolite. However, all subsequent samples, including the negative controls (**Figure 26D** and **E**) had this peak at 1.5 min which led us to conclude that this peak was an artifact of the extraction process.

While we were expecting to see polar metabolites with shorter retention times, we acknowledged the possibility that in our solvent system, the metabolite and parent compound had the same retention times. Furthermore, because quantitative analysis was not possible a decrease in peak area or peak height of propranolol could not be quantified following the metabolism studies. Rybniker et al. (2015) investigated the repurposing of lansoprazole, a proton pump inhibitor, as a candidate for use in combating *Mycobacterium tuberculosis*. During the course of their study they discovered that lansoprazole and its metabolite, lansoprazole sulfide, had the same retention time when analyzing the extracted ion chromatograms (EIC). However, mass spectrometry analysis of the single chromatogram peak, allowed them to identify molecular ions corresponding to the molecular mass of both the parent molecule and the major metabolite (Rybniker et al., 2015).

Accordingly, the sample obtained after incubation with the HEK293-CYP3A4-HA lysate was then analyzed by liquid chromatography-mass spectrometry (LC-MS), the results of which is in F**igure 27**. Previously in **Figure 3A** the mass of propranolol was reported to be 259.16 mg/mol. In **Figure 27** the molecular ion represented by a blue dot and corresponding to m/z 260.1682 is propranolol at the 1^+ charge state. After

careful analysis of the entire spectrum, no peaks could be found which matched the molecular ions of predicted metabolites (**Figure 9**). The other peaks present were attributed either to contaminants or artifacts from the extractions. Therefore, this data strongly suggests that propranolol was not metabolized after incubation with the HEK293-CYP3A4-HA lysates.

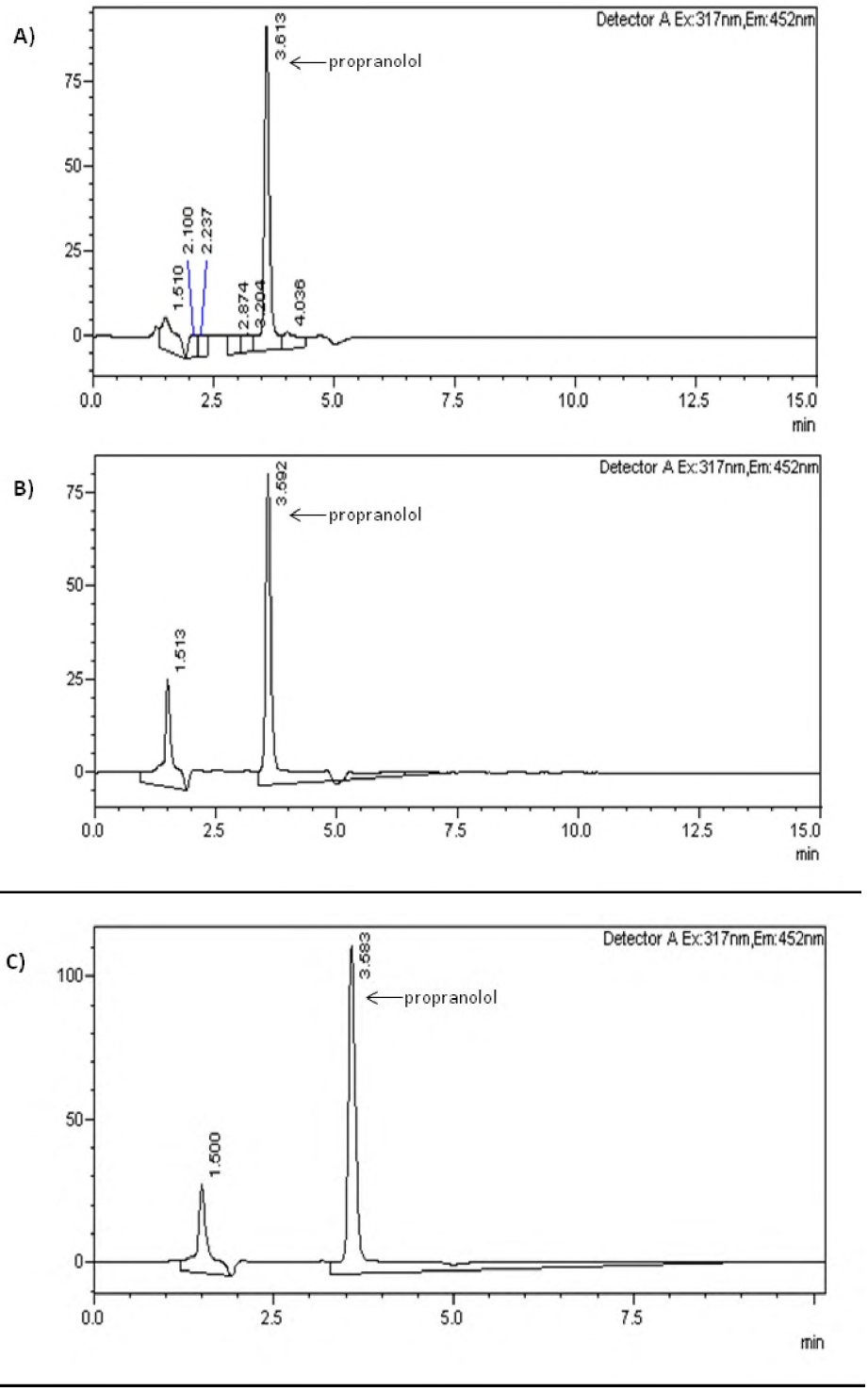

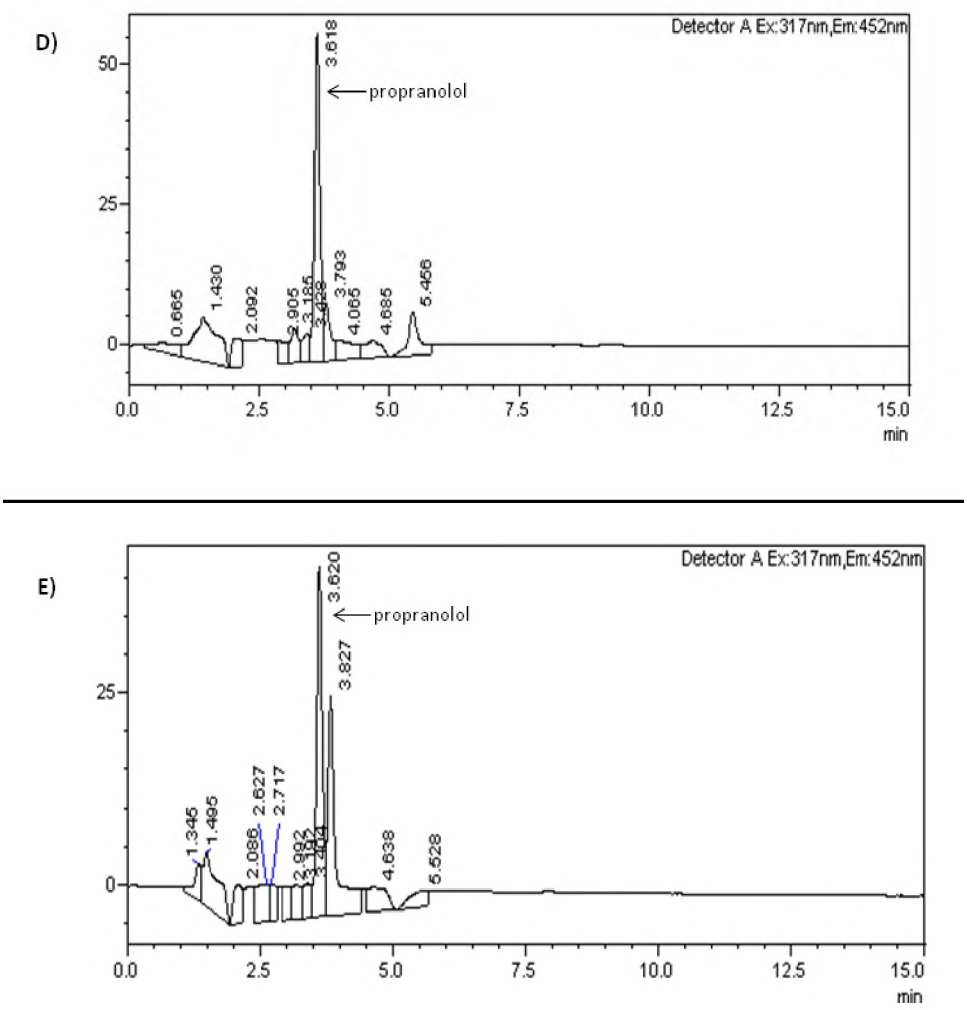

Figure 26: Metabolism and solid phase extraction of propranolol. A) *Chromatogram of propranolol at a concentration of 16 µg/ml after incubation with HEK293-CYP3A4-HA lysates and solid phase extraction.* ***B)*** *Chromatogram of propranolol at a concentration of 16 µg/ml after incubation with HEK293-pcDNA3.1+ lysates and subsequent solid phase extraction.* ***C)*** *Chromatogram of propranolol at a concentration of 16 µg/ml after incubation with untransfected HEK293 lysates and subsequent solid phase extraction.* ***D)*** *Chromatogram of propranolol at a concentration of 16 µg/ml after incubation with HEK293-CYP3A4-HA lysates but no NADPH and subsequent solid phase extraction (control).* ***E)*** *Chromatogram of propranolol at a concentration of 16 µg/ml after incubation but with no lysate present and subsequent solid phase extraction. All samples were performed in biological triplicate and a fluorescence detector was used for detection. The unit of measurement is mV. All samples were detected at Ex 317: Em 452.*

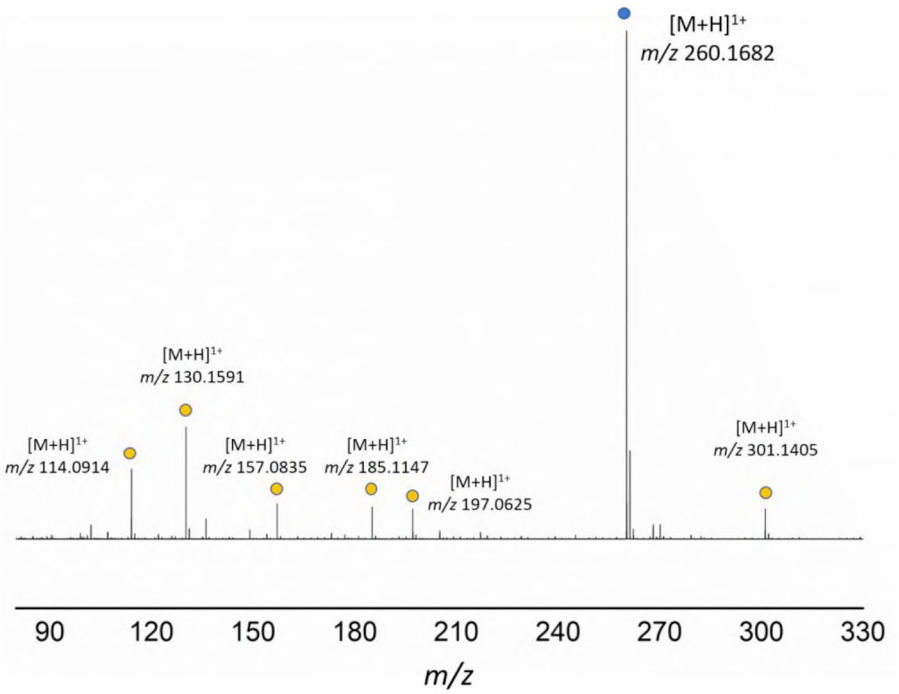

Figure 27: LC-MS data of propranolol metabolism*. The unit of measurement is m/z.*

CHAPTER 4
DISCUSSION

Main findings and results

In this study, we were interested in developing a non-hepatic cell-based platform for assessing metabolic cytotoxicity for early drug discovery. However, the use of stable cell lines, which overexpress a single CYP450 enzyme for the identification of metabolically induced cytotoxicity has been questioned as these early drug discovery studies might not provide adequate insight into the metabolic profile of a drug, even for compounds that have already been approved for use.

All four compounds which were selected for this study have been reported as inducing increased cytotoxicity in cell lines which overexpress CYP3A4. However, no change in cytotoxicity was observed in our study. While Gustafsson et al. (2014) and Rana et al. (2016) suggested that propranolol was a substrate of CYP3A4, no metabolism of propranolol was observed when using established HPLC methods, despite the activity of the CYP3A4 having been established (**Figure 20**). Furthermore, the overexpression of CYP3A4 in the HEK293 cell line resulted in increased cell proliferation (**Figure 14B**, **Figure 15**) which could possibly alter the rate of toxicity-induced cell death and result in inaccurate IC50 data.

Use of HEK293 cell line as a model for *in vitro* metabolism

We selected the HEK293 cell line to be used as a transfection host because it is easily maintained, has a quick reproduction rate and has a high efficiency of transfection (Thomas & Smart, 2005). Once a plasmid vector is introduced such as those controlled by a cytomegalovirus (CMV) it can take over the HEK293 cell's synthetic protein machinery which in turn forces the translation of the gene which had been incorporated into the plasmid (Thomas & Smart, 2005). Part of the rationale of this study was to avoid the use of hepatocytes or other hepatic cells lines due to their endogenous levels of multiple CYP450 enzymes (Gerets et al., 2012) which could result in background metabolism of the compounds and therefore may not give an accurate representation of the CYP3A4 metabolism specifically. Additionally, a study by Westerink & Schoonen (2007) found that a human hepatocellular cell line (HepG2) contained endogenous levels of Phase II enzymes which are responsible for Phase II metabolism and could contribute to the metabolism of compounds into toxic metabolites by hepatic cell lines.

The results obtained in this chapter indicated that the recombinant CYP3A4-HA enzyme was expressed in the HEK293 cell line which was shown by the presence of the HA tag through SDS-page and Western Blot analysis (**Figure 14C**). In addition, the activity of the CYP3A4 in the cells was determined by the optimization of the activity assay (**Figure 20**). In our final result for the activity assay (**Figure 20**) we observed CYP3A4 activity in the transfected pcDNA3.1+/CYP3A4-HA cell line when subtracted from background (untransfected HEK293 samples). This conclusion is based on the substrate, 7-benzyloxy-4-trifluoromethylcoumarin, being metabolized to its main metabolite which is 7-hydroxy-4-trifluoromethylcoumarin (Renwick et al., 2001). The use of this substrate was based on papers by Lu et al. (2001) and Donato, Jiménez, Castell, & Gómez-Lechón (2004). 7-Benzyloxy-4-trifluoromethylcoumarin is a known substrate for CYP3A4 and can be used to test CYP450 activity by acting as a fluorescence probe (Donato et al., 2004). However, in order to further confirm CYP3A4 activity in this transfected cell line other substrate markers such as elodipine dehydrogenase, testosterone 6 beta-hydroxylase, or midazolam 1'-hydroxylase could be utilized (Walsky & Obach, 2004).

CYP3A4 increased proliferation of HEK293 cells

Our results indicated that the transfection of the CYP3A4 into the HEK293 cell line induced proliferation as can be seen in **Figure 14B** and **Figure 15**. This phenomenon has previously been observed by Potente et al. (2002), who reported that the cell proliferation of human endothelial cells increased dramatically after the overexpression of another CYP450 enzyme, CYP2C9. The increased proliferation in this context was determined to be as a result of 11,12-EET (epoxyeicosatrienoic acid), which is a product of CYP2C9-mediated metabolism of arachidonic acid. 11,12-EET is a modulator imperative for endothelial cell homeostasis (Abukhashim, Wiebe, & Seubert, 2011). In addition, the results obtained in a study by Fedejko-sKap et al. (2011) found that overexpression of CYP3A4 in Hep3B cells increased cell growth which they believed was also due to production of 11,12-EET.

Data collected by Potente et al. (2002) indicated that the generation of 11,12-EET induces MKP-1 dephosphorylation (MAP kinase phosphatase) which is involved in cell growth (Haagenson & Wu, 2010) and the rate of dephosphorylation is increased when CYP450 enzymes are overexpressed. In addition to MKP-1 dephosphorylation, JNK (c-Jun N-terminal kinase) activity is inhibited by this signaling pathway (Potente et al., 2002). JNK activation has been associated with apoptotic response of cells to pro-

inflammatory cytokines and cell stress (Davies & Tournier, 2012). Even though JNK promotes cell survival and regulation of cell proliferation, prolonged activation of this kinase has been linked to cell apoptosis (Ventura et al., 2006). The inactivation of JNK in these cells also causes a parallel upregulation of cyclin D1, an important regulator which forms active complexes promoting cell cycle progression (Alao, 2007) (Potente et al., 2002). Therefore, a combination of increased MKP-1 dephosphorylation, inhibition of JNK and upregulation of cyclin D1 would cause an increase in endothelial cell proliferation. Importantly in the context of our study, Thuy Phuong et al. (2017) showed that 11,12-EET is also produced by CYP3A4 and therefore the CYP450 enzyme used in our study is also involved in the signaling pathway outlined above. In their study, Thuy Phuong et al. (2017) showed that the overexpression of CYP3A4 in TAMR-MCF-7 (human breast cancer cell line) cells resulted in increased cell growth and an impaired response to chemotherapy, thereby linking CYP3A4 to chemotherapy resistant breast cancer as the cells were more resilient. In both the studies mentioned above, different cell lines to that used in our study were utilized. However, Abukhashim et al. (2011) showed that HEK293 cells treated with 11,12-EET resulted in an improved response to the intracellular secondary messenger, cAMP (cyclic adenosine monophosphate). These examples illustrate that the presence of 11,12-EET in excess, which might have been produced by the overexpression of CYP3A4 in our HEK293 cells, is valuable to the function of the cell and could increase overall function, including cell proliferation. It would be interesting to evaluate the levels of 11,12-EET in the HEK293-CYP3A4-HA cell line to confirm this hypothesis. Finally, CYP3A4 also promotes the cell's progression from the G1 (gap 1) phase, in which the cells grow, to the S (synthesis) phase, when DNA is replicated, which contributes to increased tumour growth (Oguro, Sakamoto, Funae, & Imaoka, 2011).

This evidence in published literature paints a well-constructed image to explain why we observed an increase in cell proliferation upon CYP3A4 overexpression. The increased growth rate of the CYP3A4 cell line also provides further evidence that the overexpressed CYP3A4 was active.

Hypotheses for lack of observed differential toxicity between the HEK293-CYP3A4-HA and control cell lines

Based on the findings of several studies which utilized transfected hepatic cells (Gustafsson et al., 2014) (Patki et al., 2003) (Hosomi et al., 2011), we hypothesized that overexpression of CYP3A4 in the HEK293-

CYP3A4-HA cell line would result in the production of toxic metabolites leading to a dramatic decrease in cell viability compared to the control cell line. However, our results illustrate that there was no significant difference between the cell viability of the HEK293-pcDNA3.1+ and HEK293-CYP3A4-HA cell lines when treated with the same compound at equivalent concentrations (**Figures 21** and **Figure 22**).

In the study by Gustafsson et al. (2014) transformed human liver epithelial (THLE) cells where transfected with one of a variety of CYP450 enzymes, including CYP3A4. Cytotoxicity results in this study show that rosiglitazone and chlorpromazine were more toxic to the THLE cells transfected with CYP3A4 when compared to control cell lines. Gustafsson et al. (2014) attributed the observed marked increase in toxicity in the CYP3A4 transfected cell line to the presence of toxic intermediate metabolites. This study made use of a liver cell line which could be why their results do not agree with the ones obtained in our study because overexpressed CYP3A4 alone is not sufficient to produce toxic metabolites.

Hosomi et al. (2011) showed that CYP3A4 enzyme activity was significantly altered in seven immortalised hepatic cell lines. In this study several different hepatic cell lines where transfected with CYP3A4 and HepG2 cells where measured to have the highest CYP3A4 enzyme activity which they hypothesized to be as a result of endogenous levels of NADPH-P450 reductase. Additionally, this study found a decrease in viability of the CYP3A4 transfected cells when compared to control cells lines when treated with one of a variety of compounds such as terbenafine, which they hypothesize is due to the production of toxic metabolites (Hosomi et al., 2011). The variability in enzyme activity in the various hepatic cell lines indicates that there could be an even more distinguishable difference between HEK293 cells and the generally used hepatic cell lines. Therefore, the robustness of this method may be dependent on the specific conditions of a given cell line.

A study conducted by Augustin et al. (2014) reported that CYP3A4 overexpression in HepG2 cells, influenced the effect that the cytotoxic agent C-1305 had on apoptosis, necrosis and senescence, despite not directly influencing its metabolism. This indicated that the altered response of transfected HepG2 cells to C-1305 was not related to the formation of metabolites, but rather an alternative currently unknown mechanism. This article provides some valuable insight into the results obtained in our study. For example, could the increased cell proliferation have an effect on the observed lack of differential cytotoxicity? Furthermore, the cytotoxicity observed by Gustafsson et al. (2014) and Rana et al. (2016)

may not be attributed to metabolically induced toxicity. In literature, cell proliferation has had an effect on the cytotoxicity of certain compounds. The cytotoxicity of paclitaxel, an anticancer agent, for example, increases when cell growth increases (Liebmann et al., 1993). In fact, a study by Valeriote & Van Putten (1975) found that proliferating cancerous cells are more sensitive to anticancer agents than non-proliferating cells. These studies are in agreement with our hypothesis that an increase in cell proliferation could affect the cytotoxicity of certain compounds despite the fact that our CYP-expressing cell line was not more sensitive to the tested drug compounds.

It has also been reported that transfected cells could lead to an increase or decrease in the cytotoxicity of compounds even though these cells retain certain elements of normal cell growth (Lewis, Smith, Anderson, & Freshney, 1999). In the study by Lewis et al. (1999) normal human bronchial epithelial (NHBE) cells were transfected with one of nine different CYP450 enzymes. It was observed that after the introduction of the CYP450 enzymes the toxicity of some but not all mycotoxins was increased (Lewis et al., 1999), suggesting that outcomes may be different for even closely related compounds.

After the results obtained from the cytotoxicity assays it was hypothesized that the lack in toxicity could either be because there was no metabolism or that the metabolites are non-toxic. HPLC analysis confirmed that no metabolism occurred because no metabolites of propranolol were detected with HPLC analysis after incubation with lysates even though metabolites have previously been successfully detected using HPLC (Castro-Perez, 2007). This could be as a result of several factors. While a literature source has suggested that CYP3A4 is responsible for propranolol metabolism and subsequent detection of the metabolites using HPLC (Zhou, Yao, & Zeng, 2002), a study by Masubuchi et al. (1994) found that CYP2D6 and CYP1A2, rather than CYP3A4, are responsible for the production of propranolol's two main metabolites as outlined in **Scheme 4**. In fact, the results obtained in a consequent study by Johnson, Herring, Wolfe, & Relling (2000) corroborated those of Masubuchi et al. (1994) in that CYP2A6 and CYP1A2 are the main metabolic enzymes of propranolol. The possibility of propranolol not being a CYP3A4 substrate could be a reason as to why no metabolism was observed. This further highlights the shortcomings of a cell based metabolic toxicity platform. In the study by Gustafsson et al. (2014) propranolol was confirmed as a substrate of CYP3A4 due to cytotoxicity, extrapolated to be due to metabolic induced toxicity.

Limitations of study

The method of choice for our study was transgenic cell lines with recombinant human CYP450 enzymes. The reason this method was chosen for this particular study is that it is considered in literature to be the best method to generate metabolites and for use in cytotoxicity testing of drugs (Patki et al., 2003). These cell lines are easy to culture with a high yield and have an advantage over wild type cell lines in that they have a higher expression of a specific CYP450 enzyme. Therefore, the expression should be high enough to perform biotransformation studies; although these lines are quite expensive compared to other *in vitro* models (Patki et al., 2003). In addition, these cell lines theoretically allow for the study of enzymes reactions by single isoforms, such as CYP3A4. However, because only one or a few enzymes are expressed, this method is not an accurate representation of *in vivo* conditions. Additionally, in non-hepatic cell line models, because only specified CYP450 enzymes are expressed no background metabolism is present and any observed metabolism is due only to the transfected CYP450 enzymes. However, although it is impossible for *in vitro* experimental models to mimic the complexity of an entire organism, the simplicity of these models makes it possible to manipulate and analyze specific parameters. These *in vitro* studies are considered to be adequate screening mechanisms to elucidate drug metabolites and their pathways, which provides valuable information for any future *in vivo* testing (Jia & Liu, 2007). Despite the advantages it is possible that the disadvantages could be enough to discredit the use of this *in vitro* experimentation.

Other limitations of this study included using only one CYP450 enzyme for transfection and not using more than one cell line. The use of a wider range of compounds could also have given a better indication of the usefulness of this method. Future work could include transfecting cells with more than one CYP450 enzyme to observe the potential increase in metabolism and production of toxic metabolites. Furthermore, due to time constraints the method for quantitative analysis of the HPLC results was not fully developed and therefore, aspects such as decrease in peak height and peak area could not be taken into consideration when performing the metabolism studies.

Future studies

Future studies should include further development of the HPLC quantitative analysis in order to accurately determine metabolism of the parent compound. Another approach to this study would be to explore expression of CYP450 enzymes in *E.Coli* (Zydowsky, Ho, Baker, Walsh, & Mcintyre, 1992). Using *E. coli* as a host would be advantageous as it has an increased growth rate, ease in genetic manipulation, high expression of CYP450s and most importantly, it does not contain any native CYP450 which could possibly affect the measurement of the transfected CYP450 enzymes (Durairaj, Hur, & Yun, 2016).

Conclusion

When taken together, our results suggest that inferring the possibility of metabolism-induced cytotoxicity from cell based assays is unreliable. In our study, several methods of metabolism and cytotoxicity were utilized and determined to be insufficient in determining the *in silico* and *in vitro* metabolism of established compounds. We have successfully transfected CYP3A4-HA and a corresponding pcDNA3.1+ vector backbone into a HEK293 cell line as shown in **Figure 14C** and **Figure 20**. This cell line was chosen specifically due to the lack of biological CYP450 levels which are present in hepatocytes and any detection of metabolism would be solely due to the transfected CYP3A4. However, no metabolism was observed even after the activity of the CYP3A4 enzyme was proven (**Figure 20**) using a known substrate for this enzyme. Established methods were utilized in this study in order to detect metabolism, the lack of such detection points to a problem in the *in vitro* system of drug metabolism and could possibility discredit the results obtained in other studies which said otherwise.

References

Abukhashim, M., Wiebe, G. J., & Seubert, J. M. (2011). Regulation of forskolin-induced cAMP production by cytochrome P450 epoxygenase metabolites of arachidonic acid in HEK293 cells. *Cell Biology and Toxicology*, *27*(5), 321–332.

Agilent. (2013). Sample Preparation Fundamentals for Chromatography. *Agilent Presentation*, *42*(11), 2555–2568.

Agilent Technologies. (2006). How to contact Agilent Efficiently analyze your most challenging compounds. Deliver high-quality results faster. Column Selection Guide for HPLC Agilent ZORBAX Column Selection Guide for HPLC.

Alao, J. P. (2007). The regulation of cyclin D1 degradation: roles in cancer development and the potential for therapeutic invention. *Molecular Cancer*, *6*(24).

Augustin, E., Niemira, M., Hołownia, A., & Mazerska, Z. (2014). CYP3A4-dependent cellular response does not relate to CYP3A4-catalysed metabolites of C-1748 and C-1305 acridine antitumor agents in HepG2 cells. *Cell Biology International*, *38*(11), 1291–1303.

Baj-Rossi, C., De, G., & Carrar, S. (2011). P450-Based Nano-Bio-Sensors for Personalized Medicine. In *Biosensors - Emerging Materials and Applications*. InTech.

Baldwin, Clarke, & Chenery. (2001). Characterization of the cytochrome P450 enzymes involved in the in vitro metabolism of rosiglitazone. *British Journal of Clinical Pharmacology*, *48*(3), 424–432.

Banerjee, S., & Ghosh, J. (2016). Drug Metabolism and Oxidative Stress: Cellular Mechanism and New Therapeutic Insights. *Biochemistry & Analytical Biochemistry*, *5*(1).

Basheer, L., Kerem, Z., Basheer, L., & Kerem, Z. (2015). Interactions between CYP3A4 and Dietary Polyphenols. *Oxidative Medicine and Cellular Longevity*, *2015*.

Bhavani, L. R. ., & Durga, A. (2015). Method Development and Validation Parameters of HPLC- A Mini Review. *Research & Reviews: Journal of Pharmaceutical Analysis*, *4*(2).

Boehme, C. L., & Strobel, H. W. (1998). High-performance liquid chromatographic methods for the analysis of haloperidol and chlorpromazine metabolism in vitro by purified cytochrome P450 isoforms. *Journal of Chromatography B: Biomedical Sciences and Applications*, *718*(2), 259–266.

Botterblom, M. H., Feenstra, M. G., & Erdtsieck-Ernste, E. B. (1993). Determination of propranolol, labetalol and clenbuterol in rat brain by high-performance liquid chromatography. *Journal of*

Chromatography, *613*(1), 121–6.

Castro-Perez, J. M. (2007). Current and future trends in the application of HPLC-MS to metabolite-identification studies. *Drug Discovery Today*, *12*(56).

Code, E. L., Crespi, C. L., Penman, B. W., Gonzalez, F. J., Chang, T. K., & Waxman, D. J. (1997). Human cytochrome P4502B6: interindividual hepatic expression, substrate specificity, and role in procarcinogen activation. *Drug Metabolism and Disposition: The Biological Fate of Chemicals*, *25*(8), 985–93.

Crespi, C. L., & Stresser, D. M. (2000). Fluorometric screening for metabolism-based drug–drug interactions. *Journal of Pharmacological and Toxicological Methods*, *44*(1), 325–331.

Crivori, P., & Poggesi, I. (2006). Computational approaches for predicting CYP-related metabolism properties in the screening of new drugs. *European Journal of Medicinal Chemistry*, *41*(7), 795–808.

Danielson, P. B. (2002). The Cytochrome P450 Superfamily : Biochemistry , Evolution and Drug Metabolism in Humans. *Current Drug Metabolism*, *3*, 561–597.

Davies, C., & Tournier, C. (2012). Exploring the function of the JNK (c-Jun N-terminal kinase) signalling pathway in physiological and pathological processes to design novel therapeutic strategies. *Biochemical Society Transactions*, *40*(1), 85–89.

DeGrote, J., Tyndall, S., Wong, K. F., & VanAlstine-Parris, M. (2014). Synthesis of 7-alkoxy-4-trifluoromethylcoumarins via the von Pechmann reaction catalyzed by molecular iodine. *Tetrahedron Letters*, *55*(49), 6715–6717.

Denisov, I. G., Makris, T. M., Sligar, S. G., & Schlichting, I. (2005). Structure and chemistry of cytochrome P450. *Chemical Reviews*, *105*, 2253–2277.

Dolan, J. W., Snyder, L. R., & Kirkland, J. J. (2013). *Introduction to modern liquid chromatography*. Wiley.

Donato, M. T., Jiménez, N., Castell, J. V., & Gómez-Lechón, M. J. (2004). Flourescence-based assays for screening nine cytochrome p450 activities in intact cells expressing individual human P450 enzymes. *Drug Metabolism and Disposition*, *32*(7), 699–706.

Du, Y., Wang, J., Jia, J., Song, N., Xiang, C., Xu, J., … Deng, H. (2014). Human Hepatocytes with Drug Metabolic Function Induced from Fibroblasts by Lineage Reprogramming. *Cell Stem Cell*, *14*(3), 394–403.

Durairaj, P., Hur, J.-S., & Yun, H. (2016). Versatile biocatalysis of fungal cytochrome P450 monooxygenases. *Microbial Cell Factories*, *15*(1).

Fasinu, P., Bouic, P. J., & Rosenkranz, B. (2012). Liver-Based In Vitro Technologies for Drug

Biotransformation Studies -A Review. *Current Drug Metabolism*, *13*.

Fedejko-Kap, B., Niemira, M., Radominska-Pandya, A., & Mazerska, Z. (2011). Flavin monooxygenases, FMO1 and FMO3, not cytochrome P450 isoenzymes, contribute to metabolism of anti-tumour triazoloacridinone, C-1305, in liver microsomes and HepG2 cells. *Xenobiotica*, *41*(12), 1044–1055.

Gal, J., Zirrolli, J. A., & Lichtenstein, P. S. (1988). Labetalol is metabolized oxidatively in humans. *Research Communications in Chemical Pathology and Pharmacology*, *62*(1), 3–17.

Gerets, H. H. J., Tilmant, K., Gerin, B., Chanteux, H., Depelchin, B. O., Dhalluin, S., … Chanteux, : H. (2012). Characterization of primary human hepatocytes, HepG2 cells, and HepaRG cells at the mRNA level and CYP activity in response to inducers and their predictivity for the detection of human hepatotoxins. *Cell. Biol. Toxicol.*, *28*, 69–87.

Gheshlaghi, R., Scharer, J. M., Moo-Young, M., & Douglas, P. L. (2008). Application of statistical design for the optimization of amino acid separation by reverse-phase HPLC. *Analytical Biochemistry*, *383*, 93–102.

Gibson, G., & Skett, P. (2001). *Introduction to Drug Metabolism* (3rd ed.). London: Nelson Thornes Publishers.

Gomez-Lechon, M., Donato, M., Castell, J., & Jover, R. (2003). Human Hepatocytes as a Tool for Studying Toxicity and Drug Metabolism. *Current Drug Metabolism*, *4*(4), 292–312.

Goulding, R., & Marden, E. (2009). An Overview of Drug Discovery and Drug Development.

Guengerich, F. P. (2006). Cytochrome P450s and other enzymes in drug metabolism and toxicity. *The AAPS Journal*, *8*(1), 101–111.

Guillén, M. I., Donato, M. T., Jover, R., Castell, J. V, Fabra, R., Trullenque, R., & Gómez-Lechón, M. J. (1998). Oncostatin M down-regulates basal and induced cytochromes P450 in human hepatocytes. *The Journal of Pharmacology and Experimental Therapeutics*, *285*(1), 127–34.

Gunaratna, C. (2000). Drug Metabolism & Pharmacokinetics in Drug Discovery: A Primer for Bioanalytical Chemists, Part 1. *Current Separations*, *19*(1).

Gupta, R. P., Hollis, B. W., Patel, S. B., Patrick, K. S., & Bell, N. H. (2003). CYP3A4 is a Human Microsomal Vitamin D 25-Hydroxylase. *Journal of Bone and Mineral Research*, *19*(4), 680–688.

Gustafsson, F., Foster, A. J., Sarda, S., Bridgland-Taylor, M. H., & Kenna, J. G. (2014). A correlation between the in vitro drug toxicity of drugs to cell lines that express human P450s and their propensity to cause liver injury in humans. *Toxicological Sciences : An Official Journal of the Society of Toxicology*, *137*(1), 189–211.

Haagenson, K. K., & Wu, G. S. (2010). The role of MAP kinases and MAP kinase phosphatase-1 in resistance to breast cancer treatment. *Cancer Metastasis Reviews*, *29*(1), 143–9.

Haddad, P. R., Drouen, A. C. J. H., Billiet, H. A. H., & De Galan, L. (1983). Combined optimization of mobile phase pH and organic modifier content in the separation of some aromatic acids by reversed-phase high-performance liquid chromatography. *Journal of Chromatography*, *282*, 71–81.

Hawes, E. M., Jaworski, T. J., Midha, K. K., McKay, G., Hubbard, J. W., & Korchinski, E. D. (1991). In vivo metabolism of N-oxides. In *N-Oxidation of Drugs* (pp. 263–286). Dordrecht: Springer Netherlands.

Hedeen, K. M., Tyczkowska, K., Aucoin, D. P., & Norton, R. M. (1991). Rapid high-performance liquid chromatographic method for the determination of propranolol levels in canine and feline plasma. *Journal of Chromatography*, *572*(1–2), 239–45.

Hosomi, H., Fukami, T., Iwamura, A., Nakajima, M., Yokoi, T., & Yokoi, T. (2011). Development of a highly sensitive cytotoxicity assay system for CYP3A4-mediated metabolic activation. *Drug Metabolism and Disposition: The Biological Fate of Chemicals*, *39*(8), 1388–95.

Hughes, J. P., Rees, S., Kalindjian, S. B., & Philpott, K. L. (2011). Principles of early drug discovery. *British Journal of Pharmacology*, *162*(6), 1239–49.

Humma, L. M., Ellingrod, V. L., & Kolesar, J. M. (2003). *Lexi-Comp's pharmacogenomics handbook*. Lexi-Comp.

Jia, L., & Liu, X. (2007). The conduct of drug metabolism studies considered good practice (II): in vitro experiments. *Current Drug Metabolism*, *8*(8), 822–9.

Johnson, J. A., Herring, V. L., Wolfe, M. S., & Relling, M. V. (2000). CYP1A2 and CYP2D6 4-Hydroxylate Propranolol and Both Reactions Exhibit Racial Differences 1. *The Journal of Pharmacology and Experimental Therapeutics*, *294*, 1099–1105.

Keglevich, G., Bálint, E., Karsai, É., Grün, A., Bálint, M., & Greiner, I. (2008). Chemoselectivity in the microwave-assisted solvent-free solid–liquid phase benzylation of phenols: O-versus C-alkylation. *Tetrahedron Letters*, *49*, 5039–5042.

Keserű, G. M., & Makara, G. M. (2006). Hit discovery and hit-to-lead approaches. *Drug Discovery Today*, *11*(15), 741–748.

Kim, H. K., Hong, J. H., Park, M. S., Kang, J. S., & Lee, M. H. (2001). Determination of propranolol concentration in small volume of rat plasma by HPLC with fluorometric detection. *Biomedical Chromatography*, *15*(8), 539–545.

Kirchmair, J., Göller, A. H., Lang, D., Kunze, J., Testa, B., Wilson, I. D., … Schneider, G. (2015). Predicting

drug metabolism: experiment and/or computation? *Nature Reviews. Drug Discovery*, *14*(6), 387–404.

Lacey, C. F., Armstrong, L. L., & Goldman, M. P. (2007). *Drug Information Handbook* (15th ed.). Hudson: Lexi-Comp.

Laemmli, U. . (1970). Cleavage of Structural Proteins during the Assembly of the Head of Bacteriophage T4. *Nature*, *227*(5259), 680–685.

Lewis, C. W., Smith, J. E., Anderson, J. G., & Freshney, R. I. (1999). Increased cytotoxicity of food-borne mycotoxins toward human cell lines in vitro via enhanced cytochrome p450 expression using the MTT bioassay. *Mycopathologia*, *148*, 97–102.

Liebmann, J. E., Cook, J. A., Lipschultz, C., Teague, D., Fisher, J., & Mitchell, J. B. (1993). Cytotoxic studies of pacfitaxel (Taxol®) in human tumour cell lines. *Br. J. Cancer*, *68*, 1104–1109.

Lu, P., Lin, Y., Rodrigues, A. D., Rushmore, T. H., Baillie, T. A., & Shou, M. (2001). Testosterone, 7-Benzyloxyquinoline, and 7-Benzyloxy-4-trifluoromethyl-coumarin Bind to Different Domains within the Active Site of Cytochrome P450 3A4. *Drug Metabolism and Disposition*, *29*(11).

Lynch, T., & Price, A. (2007). The Effect of Cytochrome P450 Metabolism on Drug Response, Interactions, and Adverse Effects. *American Family Physician*, *76*(1), 391–396.

Masubuchi, Y., Hosokawa, S., Horie, T., Suzuki, T., Ohmori, S., Kitada, M., & Narimatsu, S. (1994). Cytochrome P450 isozymes involved in propranolol metabolism in human liver microsomes. The role of CYP2D6 as ring-hydroxylase and CYP1A2 as N-desisopropylase. *Drug Metabolism and Disposition: The Biological Fate of Chemicals*, *22*(6), 909–15.

Maurer, S. M. (2006). Choosing the right incentive strategy for research and development in neglected diseases. *Bulletin of the World Health Organization*, *84*(5), 376–381.

Murayama, N., Sai, K., Nakajima, Y., Kaniwa, N., Ozawa, S., Ohno, Y., & Sawada, J. (2001). Expression of CYP2A6 in tumor cells augments cellular sensitivity to tegafur. *Japanese Journal of Cancer Research*, *92*(5), 524–8.

Narimatsu, S., Arai, T., Watanabe, T., Masubuchi, Y., Horie, T., Suzuki, T., … Cho, A. K. (1997). Covalent Binding of a Reactive Metabolite Derived from Propranolol and Its Active Metabolite 4-Hydroxypropranolol to Hepatic Microsomal Proteins of the Rat. *Chemical Research in Toxicology*, *10*, 289–295.

Ogu, C. C., & Maxa, J. L. (2000). Drug interactions due to cytochrome P450. *Pharmacology Notes*, *13*(4), 421–3.

Oguro, A., Sakamoto, K., Funae, Y., & Imaoka, S. (2011). Overexpression of CYP3A4, but not of CYP2D6, Promotes Hypoxic Response and Cell Growth of Hep3B Cells. *Drug Metabolism and Pharmacokinetics*, *26*(4), 407–15.

Oscarson, M., McLellan, R. A., Asp, V., Ledesma, M., Ruiz, M. L. B., Sinues, B., … Ingelman-Sundberg, M. (2002). Characterization of a novelCYP2A7/CYP2A6 hybrid allele (CYP2A6*12) that causes reduced CYP2A6 activity. *Human Mutation*, *20*(4), 275–283.

Park, K., Williams, D. P., Naisbitt, D. J., Kitteringham, N. R., & Pirmohamed, M. (2005). Investigation of toxic metabolites during drug development. *Toxicology and Applied Pharmacology*, *207*(2), 425–434.

Patki, K. C., Moltke, L. L. von, & Greenblatt, D. J. (2003). In vitro metabolism of midazolam, triazolam, nifedipine, and testosterone by human liver microsomes and recombinant cytochromes P450: role of CYP3A4 and CYP3A5. *Drug Metabolism and Disposition*, *31*(7), 938–944.

Pires, D. E. V, Blundell, T. L., & Ascher, D. B. (2015). pkCSM: Predicting Small-Molecule Pharmacokinetic and Toxicity Properties Using Graph-Based Signatures. *Journal of Medicinal Chemistry*, *58*(9), 4066–72.

Pirok, G. (2013). ChemAxon Metabolizer.

Potente, M., Michaelis, U. R., Fisslthaler, B., Busse, R., & Fleming, I. (2002). Cytochrome P450 2C9-induced endothelial cell proliferation involves induction of mitogen-activated protein (MAP) kinase phosphatase-1, inhibition of the c-Jun N-terminal kinase, and up-regulation of cyclin D1. *The Journal of Biological Chemistry*, *277*(18), 15671–6.

Rana, P., Will, Y., Nadanaciva, S., & Jones, L. H. (2016). *Development of a cell viability assay to assess drug metabolite structure–toxicity relationships*. *Bioorganic & Medicinal Chemistry Letters* (Vol. 26).

Ray, W. A., Murray, K. T., Meredith, S., Narasimhulu, S. S., Hall, K., & Stein, C. M. (2004). Oral Erythromycin and the Risk of Sudden Death from Cardiac Causes. *New England Journal of Medicine*, *351*(11), 1089–1096.

Renwick, A. B., Lewis, D. F. V., Fulford, S., Surry, D., Williams, B., Worboys, P. D., … Evans, D. C. (2001). Metabolism of 2,5-bis(trifluoromethyl)-7-benzyloxy-4-trifluoromethylcoumarin by human hepatic CYP isoforms: evidence for selectivity towards CYP3A4. *Xenobiotica*, *31*(4), 187–204.

Ridley, D. B., Grabowski, H. G., & Moe, J. L. (2006). Developing Drugs For Developing Countries Linking incentives for essential drugs in developing countries with blockbuster drugs in the developed world would help both achieve better population health. *Health Affairs*, *25*(10), 313–324.

Rousu, & Timo. (2012). Liquid chromatography-mass spectrometry in drug metabolism studies. *A Scientiae Rerum Naturalium*, *594*.

Rurak, D. W., Yeleswaram, K., Kwan, E., Hall, C., Doroudian, A., Abbott, F. S., & Axelson, J. E. (1992). Disposition, metabolism, and pharmacodynamics of labetalol in adult sheep. *Drug Metabolism and Disposition*, *21*(2), 284–292.

Rybniker, J., Vocat, A., Sala, C., Busso, P., Pojer, F., Benjak, A., & Cole, S. T. (2015). Lansoprazole is an antituberculous prodrug targeting cytochrome bc1. *Nature Communications*, *6*.

Sacks, L. V., Shamsuddin, H. H., Yasinskaya, Y. I., Bouri, K., Lanthier, M. L., & Sherman, R. E. (2014). Scientific and Regulatory Reasons for Delay and Denial of FDA Approval of Initial Applications for New Drugs, 2000-2012. *JAMA*, *311*(4), 378–384.

Sawadaa, M., & Kamatakib, T. (1998). Genetically engineered cells stably expressing cytochrome P450 and their application to mutagen assays. *Mutation Research/Reviews in Mutation Research*, *411*(1), 19–43.

Schenone, M., Dančík, V., Wagner, B. K., & Clemons, P. A. (2013). Target identification and mechanism of action in chemical biology and drug discovery. *Nature Chemical Biology*, *9*(4), 232–240.

Scott, E. E., & Halpert, J. R. (2005). Structures of cytochrome P450 3A4. *Trends in Biochemical Sciences*, *30*(1), 5–7.

Shih, H., Pickwell, G. V, Guenette, D. K., Bilir, B., & Quattrochi, L. C. (1999). Species differences in hepatocyte induction of CYP1A1 and CYP1A2 by omeprazole. *Human & Experimental Toxicology*, *18*(2), 95–105.

Shimadzu. (2017a). Differences Between Using Acetonitrile and Methanol for Reverse Phase Chromatography.

Shimadzu. (2017b). Tips for practical HPLC analysis. *LC World Talk*, *2*.

Snyder, L. R., Kirkland, J. J. (Joseph J., & Glajch, J. L. (1997). *Practical HPLC method development*. Wiley.

Spracklin, D. K., Hankins, D. C., Fisher, J. M., Thummel, K. E., & Kharasch, E. D. (1997). Cytochrome P450 2E1 is the Principal Catalyst of Human Oxidative Halothane Metabolism in Vitro 1. *The Journal of Pharmacology and Experimental Therapeutics*, *281*, 400–411.

Sridar, C., Kent, U. M., Noon, K., McCall, A., Alworth, B., Foroozesh, M., & Hollenberg, P. F. (2008). Differential inhibition of cytochromes P450 3A4 and 3A5 by the newly synthesized coumarin derivatives 7-coumarin propargyl ether and 7-(4-trifluoromethyl)coumarin propargyl ether. *Drug Metabolism and Disposition: The Biological Fate of Chemicals*, *36*(11), 2234–43.

Swartz, M. (2010). HPLC Detectors: A Brief Review. *Journal of Liquid Chromatography and Related Technologies*, *33*, 1130–1150.

Thomas, P., & Smart, T. G. (2005). HEK293 cell line: A vehicle for the expression of recombinant proteins. *Journal of Pharmacological and Toxicological Methods*, *51*(3), 187–200.

Thuy Phuong, N. T., Kim, J. W., Kim, J.-A., Jeon, J. S., Lee, J.-Y., Xu, W. J., … Kang, K. W. (2017). Role of the CYP3A4-mediated 11,12-epoxyeicosatrienoic acid pathway in the development of tamoxifen-resistant breast cancer. *Oncotarget*, *8*(41), 71054–71069.

Towbin, H., Staehelin, T., & Gordon, J. (1979). Electrophoretic transfer of proteins from polyacrylamide gels to nitrocellulose sheets: procedure and some applications. *Proceedings of the National Academy of Sciences of the United States of America*, *76*(9), 4350–4.

Tyndall, S., Wong, K. F., & VanAlstine-Parris, M. A. (2015). Insight into the Mechanism of the Pechmann Condensation Reaction Using NMR. *The Journal of Organic Chemistry*, *80*(18), 8951–8953.

Valeriote, F., & Van Putten, L. (1975). Proliferation-dependent Cytotoxicity of Anticancer Agents: A Review i. *Cancer Research*, *35*, 2619–2630.

Velasco, R., Silva López, C., Nieto Faza, O., & Sanz, R. (2016). Exploring the Reactivity of α-Lithiated Aryl Benzyl Ethers: Inhibition of the [1,2]-Wittig Rearrangement and the Mechanistic Proposal Revisited. *Chemistry - A European Journal*, *22*(42), 15058–15068.

Ventura, J.-J., Hübner, A., Zhang, C., Flavell, R. A., Shokat, K. M., & Davis, R. J. (2006). Chemical Genetic Analysis of the Time Course of Signal Transduction by JNK. *Molecular Cell*, *21*(5), 701–710.

Vignati, L., Turlizzi, E., Monaci, S., Grossi, P., De Kanter, R., & Monshouwer, M. (2005). An in vitro approach to detect metabolite toxicity due to CYP3A4-dependent bioactivation of xenobiotics. *Toxicology*, *216*, 154–167.

Walsky, R. L., & Obach, R. S. (2004). Validated assays for human cytochrome P450 activities. *Drug Metabolism and Disposition*, *32*(6), 647–660.

Wang, J., & Urban, L. (2004). The impact of early ADME profiling on drug discovery and development strategy. *Drug Discovery World*, 73–86.

Wang, R. W., Newton, D. J., Scheri, T. D., Lu, A. Y., Lu, A., Zhang, Y., … Baillie, T. (1997). Human cytochrome P450 3A4-catalyzed testosterone 6 beta-hydroxylation and erythromycin N-demethylation. Competition during catalysis. *Drug Metabolism and Disposition: The Biological Fate of Chemicals*, *25*(4), 502–7.

Westerink, W. M. A., & Schoonen, W. G. E. J. (2007). Phase II enzyme levels in HepG2 cells and

cryopreserved primary human hepatocytes and their induction in HepG2 cells. *Toxicology in Vitro*, *21*(8), 1592–1602.

Wu, J., Diao, T., Sun, W., & Li, Y. (2006). Expeditious Approach to Coumarins via Pechmann Reaction Catalyzed by Molecular Iodine or AgOTf. *Synthetic Communications*, *36*(20), 2949–2956.

Xie, S.-S., Wang, X., Jiang, N., Yu, W., Wang, K. D. G., Lan, J.-S., … Kong, L.-Y. (2015). Multi-target tacrine-coumarin hybrids: Cholinesterase and monoamine oxidase B inhibition properties against Alzheimer's disease. *European Journal of Medicinal Chemistry*, *95*, 153–165.

Yamane, M., Kawashima, K., Yamaguchi, K., Nagao, S., Sato, M., Suzuki, M., … Ishigai, M. (2015). Xenobiotica the fate of foreign compounds in biological systems In vitro profiling of the metabolism and drug–drug interaction of tofogliflozin, a potent and highly specific sodium-glucose co-transporter 2 inhibitor, using human liver microsomes, human he. *Xenobiotica*, *45*(3), 1366–5928.

Youdim, M. B. H., & Riederer, P. F. (2004). A review of the mechanisms and role of monoamine oxidase inhibitors in Parkinson's disease. *Neurology*, *63*(Issue 7, Supplement 2), S32–S35.

Zhou, Q., Yao, T. W., & Zeng, S. (2002). Chiral reversed phase high-performance liquid chromatography for determining propranolol enantiomers in transgenic Chinese hamster CHL cell lines expressing human cytochrome P450. *J. Biochem. Biophys. Methods*, *54*, 369–376.

Zydowsky, L. D., Ho, S. I., Baker, C. H., Walsh, C. T., & Mcintyre, K. (1992). Overexpression, purification, and characterization of yeast cyclophilins A and B. *Protein Science*, *1*(8), 961–969.